*Thesis*

*On*

# MULTI-RESPONSE OPTIMIZATION OF PROCESS PARAMETERS IN COLD CHAMBER PRESSURE DIE CASTING

*Submitted in partial fulfillment of the requirement for the award of the degree of*

**Master of Engineering**

**IN**

**PRODUCTION & INDUSTRIAL ENGINEERING**


*Submitted By*

**LALIT KUMAR**

**Roll No. 80782501**


Under the Guidance of


Dr. Ajay Batish
Associate Professor
Thapar University, Patiala

Mr. Anirban Bhattacharya
Assistant Professor
Thapar University, Patiala



DEPARTMENT OF MECHANICAL ENGINEERING

THAPAR UNIVERSITY

PATIALA-147004, INDIA

## DECLARATION

This is to certify that the thesis entitled **"Multi-Response Optimization of Process Parameters in Cold Chamber Pressure Die Casting"** is an authentic record of my study carried out as requirements for the award of the degree of **Master of Engineering in Mechanical (Production and Industrial) Engineering** to **Thapar University, Patiala,** under the guidance of **Dr. AJAY BATISH**, Associate Professor and **Mr. ANIRBAN BHATTACHARYA,** Assistant Professor Department of Mechanical Engineering, Thapar University, Patiala during **July 2009 to July 2010.** This matter embodied in this thesis has not been submitted in part or full to any other university or institute for the award of any degree.

**Lalit Kumar**

This is to certify that above declaration made by the student concerned is correct to the best of my knowledge & belief.

15/7/10

**(Dr. AJAY BATISH)**
Associate Professor,
Thapar University,
Patiala, 147004.

**(ANIRBAN BHATTACHARYA)**
Assistant Professor,
Thapar University,
Patiala, 147004.

*Countersigned by:*

**(Dr. S.K. MOHAPATRA)**
Professor & Head,
Department of Mechanical Engineering,
Thapar University, Patiala, 147004.

**(Dr.R.K. SHARMA)**
Dean of Academic Affairs,
Thapar University,
Patiala, 147004.

# ABSTRACT

Die casting are amongst the highest volume, mass produced items manufactured by the metalwork industry, and they can be found in thousands of consumer, commercial and industrial products Aluminium alloy is light in weight, while processing high dimensional stability for complex shapes and thin walls. The objective of the study was to evaluate the main effects i.e. thermal characteristics (temperature of the molten metal), injection pressure of the molten metal, type of coating (oil coating, oil + graphite coating, dycot coating), and the type of cooling (air cooling, water cooling and oil cooling) on density of the material, hardness of the material and the surface roughness of the material. An experimental model for MRSN ratio encompassing three responses namely surface roughness, density and hardness has been employed to carry out the experimental study and subsequent analysis. ANOVA was performed for all the responses and the effect of the factors was explained with the help of main effect plots. Regression analysis was done to correlate the affect of factors with all the three responses. Micro structural analysis for all the trials was done. In the end MRSN was done to optimise the responses and regression equation was developed to predict the MRSN values.

## ACKNOWLEDGEMENTS

With deep sense of gratitude I express my sincere thanks to my guides, ***Dr. Ajay Batish*** , and ***Mr. Anirban Bhattacharya*** for their valuable guidance, proper advice and constant encouragement during the my thesis work from the initial level to final level. I also feel very much obliged to ***Dr. S.K. Mohapatra***, Professor & Head, of Mechanical Engineering Department.

I would like to thanks all the members and employees of Mechanical Engineering Department, Thapar University, Patiala for their everlasting support.

I am also very thankful to my friends for their cooperation.

I offer my regards to all of those who supported me in any respect during the completion of the work.

Lastly, and most importantly, I wish to thank my parents, my wife and children. They supported me and loved me. To them I dedicate this thesis.

**LALIT KUMAR**

**Registration No. 80782501**

**INDEX**

# LIST OF FIGURES

# LIST OF TABLES

# CHAPTER 1

# COLD CHAMBER DIECASTING

## 1.1 INTRODUCTION

Die casting are amongst the highest volume, mass produced items manufactured by the metalwork industry, and they can be found in thousands of consumer, commercial and industrial products. Die cast parts are important components of product ranging from automobiles to toys. Parts can be as simple as sink faucet or as complex as connector housing. Die casting is one of the fastest and most cost-effective methods for producing a wide range of components. However, to achieve maximum benefits from this process, it is critical that designers collaborate with the die caster at an early stage of the product design and development. Consulting with the die caster during the design phase will help resolve issues affecting tooling and production, while identifying the various trade-offs that could affect overall costs. For instance, the parts having external undercuts or projections on sidewalls often require dies with slides. Slides increase the cost of the tooling, but may result in reduced metal use, uniform casting wall thickness or other advantages. These savings may offset the cost of tooling, depending upon the production quantities, providing overall economies [1].

Die-casting is similar to permanent mold casting except that the metal is injected into the mold under *high pressure* of 10-210Mpa. This results in a more uniform part, generally good surface finish and good dimensional accuracy which is as good as 0.2 % of the linear dimension. For many parts, post-machining can be totally eliminated or very light machining may be required to bring dimensions to size [2].

## 1.2 HISTORY

The earliest example of die casting by pressure injection- as opposed to casting by gravity pressure occurred in the mid 1800s. A patent was awarded to Sturges in 1849 [1] for the first manually operated machine for casting printing type. The application was limited to printer's type for the next 20 years, but development of other shapes began to increase towards the end of century. By 1892, commercial application including parts of photographs and cash register, and mass production of many types of parts began in the early 1900s. The first die

casting alloy were various compositions of tin and lead, but their use declined with the introduction of zinc and aluminium alloy in 1914. Magnesium and copper alloys quickly followed and by 1930s, many of modern alloys still used today became available. The casting process has evolved from the original low pressure injection method to techniques including high pressure casting at forces exceeding 4500 pounds per square inch (psi). These modern processes are capable of producing integrity, near net shape casting with excellent surface finish [1].

### 1.1.2 The Future of Die Casting

Continuous refinement in both the alloy used in die casting and the process itself, has expanded the die casting applications into almost every known market. Once limited to only lead, today's die caster can produce casting in variety of sizes shapes and wall thickness that are strong durable and dimensionally precise [1].

## 1.3 ADVANTAGES OF DIE CASTING

Die casting is an efficient, economical process offering a wide range of shapes and components than any other manufacturing techniques. Parts have long service life and may be designed to compliment visual appeal of the surrounding parts. Designer can gain a number of advantages and benefits by specifying die casting parts. The other advantage of die casting includes:-

### 1.3.1 High Speed Production

Die casting provides complex shapes within closer tolerances than any other mass production process. Little or no machining is required and thousand of identical parts can be produced before additional tooling is required.

### 1.3.2 Dimensional Accuracy and Stability

Die casting produces parts that are durable and dimensionally stable, while maintaining close tolerances. They are also heat resistant.

### 1.3.3 Strength and Weight

Die cast parts are stronger than plastic injection molded parts having the same dimensions. Thin walls castings are stronger and lighter than those possible with other casting method. (Plus die cast products do not require separate parts to be welded or fastened together and the strength is that of the alloy is greater than the joining processes).

### 1.3.5 Multiple Finishing Techniques

Die cast parts can be produced with smooth or textured surface and they are easily plated or finished with a minimum of surface preparation.

### 1.3.6 Simplified Assembly

Die casting provides integrated fastening elements such as bosses and studs. Holes can be cored and made to tap drill size or external threads can be cast. [1]

## 1.4 DIE CASTING PROCESS

The basic die casting process consists of injecting the molten metal under high pressure into a steel mould called a die. Die casting machines are typically rated in clamping tons equal to the pressure they can exert on the die. Machine size ranges from 400 tons to 4000 tons. Regardless of their sizes the only fundamental difference in die casting machine is the method used to inject molten metal into a die. The two methods are

- Hot chamber
- Cold chamber die casting.

### 1.4.1 Hot Chamber Die Casting Process:

Hot chamber machines are used primarily for zinc, copper, magnesium, lead and other low melting point alloys that do not readily attack and erode metal pots, cylinders and plungers. The injection mechanism of a hot chamber machine is immersed in the molten metal bath of a metal holding furnace. The furnace is attached to the machine by a metal feed system called a gooseneck. As the injection cylinder plunger rises, a port in the injection cylinder opens, allowing molten metal to fill the cylinder. As the plunger moves downward it seals the port and forces molten metal through the gooseneck and nozzle into the die cavity. After the metal

has solidified in the die cavity, the plunger is withdrawn, the die opens and the casting is ejected.

A complete die casting cycle can vary from one second for small component weighing less than one ounce to three minutes for a casting of several pounds. This makes the die casting process the faster technique for producing precise non ferrous metal parts. [1]. The schematic of the process is shown in Figure1.1.

***Hot-chamber die casting cycle process:***

- With die closed and plunger withdrawn, molten metal flows into the chamber.
- Plunger forces metal in chamber to flow into die, maintaining pressure during cooling and solidification.
- Plunger is withdrawn, die is opened, and solidified part is ejected.
- Finished part is shown in Figure 1.1 (4)

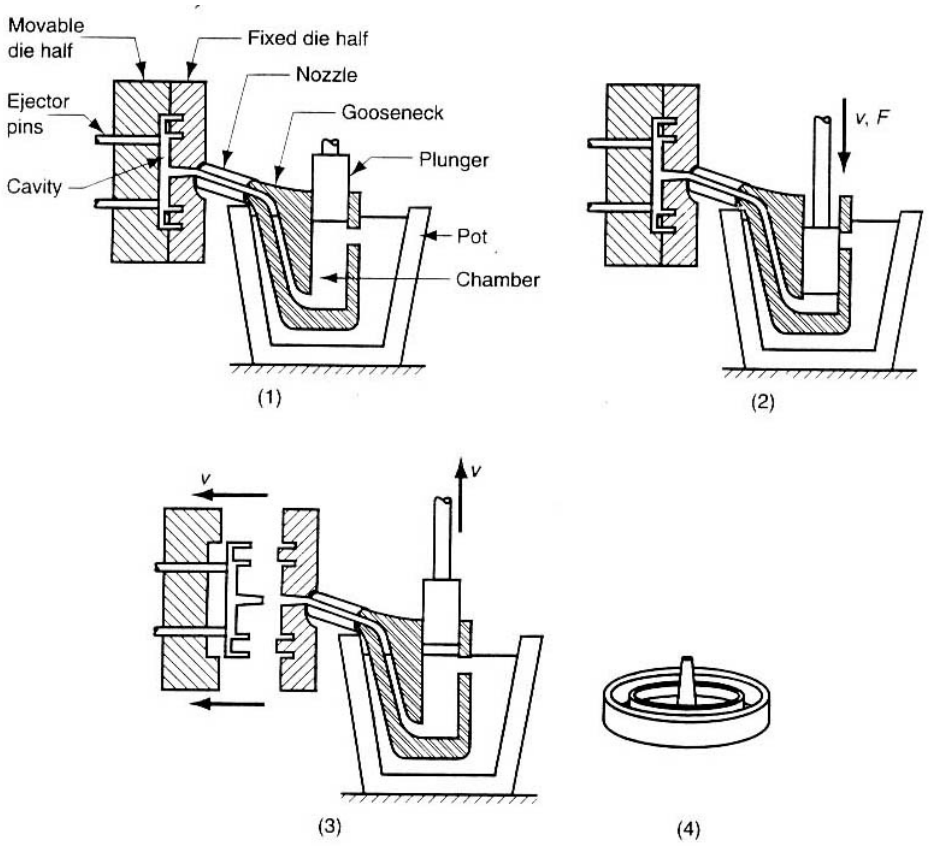


Figure 1.1 Hot Chamber Die Casting Machine [1]

### 1.4.2 Cold Chamber Die Casting Process

The cold chamber die casting process is used with higher-melting-point alloys, such as aluminum and magnesium. Since the cold chamber is located outside of the furnace, as compared to hot chamber, it requires a means of moving the molten metal from the holding furnace to the cold chamber. The cold chamber is attached between the die casting machine front platen and the die. The transport of the molten metal is typically done with a ladle mechanism, either manually or automatically, when casting aluminum alloys. Casting cycle times can range from 10 s for a small machine to 2 min for a large machine [3].

In cold chamber process, the molten metal is ladled into the cold chamber for each shot, as shown in Figure 1.2. There is less time exposure of the melt to the plunger walls or the plunger. This is particularly useful for metals such as Aluminium, copper and its alloys that alloys easily with iron at higher temperatures**.** Die casting molds tend to be expensive as they are made from hardened steel, also the cycle time for building these is long. The stronger and harder metals such as iron and steel cannot be die cast [2].

***Cold-chamber die casting process cycle***

- With die closed and plunger withdrawn, molten metal is poured into the chamber;
- Plunger forces metal to flow into die, maintaining pressure during the cooling and solidification; and
- Plunger is withdrawn, die is opened, and part is ejected. Used for higher temperature metals e.g. Aluminium, Copper and their alloys.

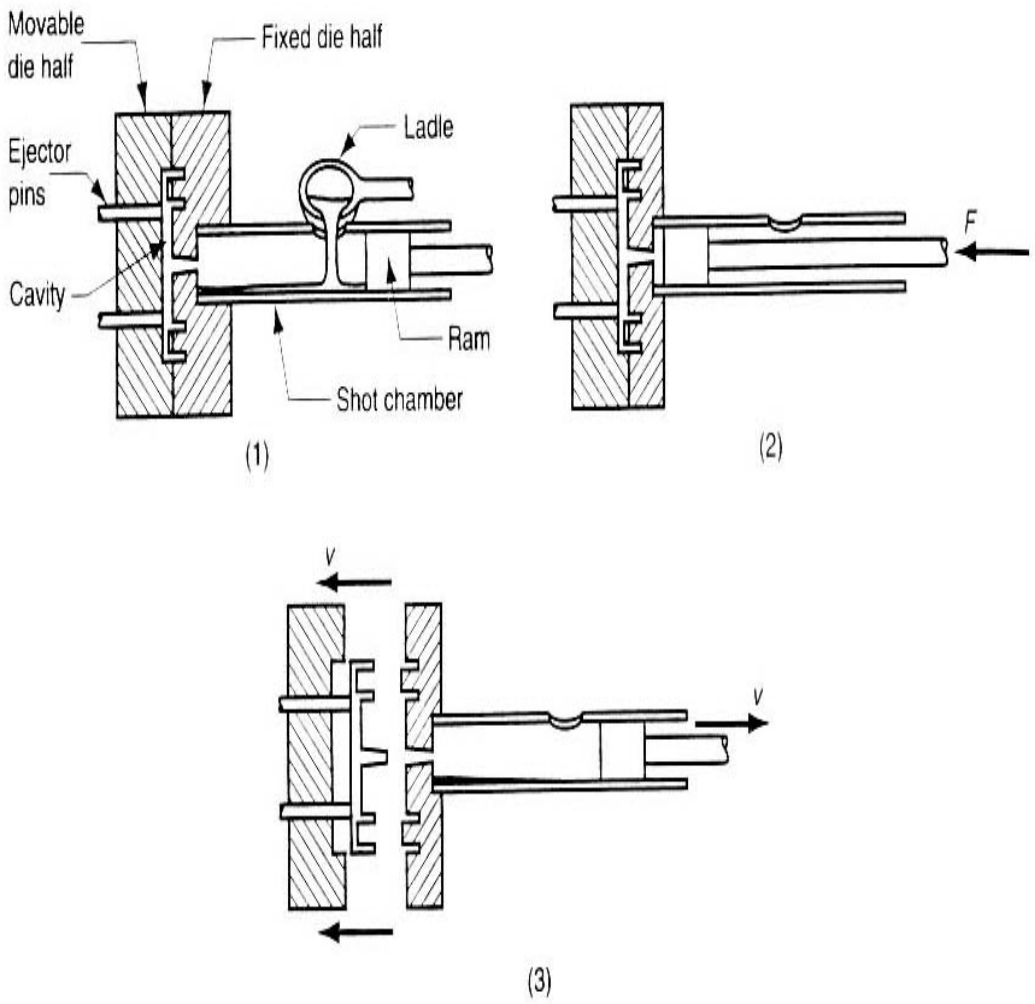


Figure 1.2 Cold chamber die casting process cycle [1]

## 1.5 DIE CONSTRUCTION

Dies or die casting tooling are made of alloy tool steel in at least two sections, one is fixed die half or cover half and the ejector die half, to permit the removal of casting.

Modern dies also may have moveable slides, cores or other section to produce holes, threads and other desired shapes in casting. Sprue hole is in the fixed die that allows the molten metal to enter the die and fill the cavity. The fixed die usually contain the runner (passage way) and gates (inlet) that route the molten metal to the die cavity. Dies also includes locking pins to secure the two halves, ejector pins to help remove the cast part and opening for coolant and lubricants. When the die casting machine closes, the two die halves are locked and held

together by the machines hydraulic pressure. The surface where the ejector and fixed die halves of the die meet and locked is referred as die parting line. The total projected surface area of the part being cast, measured at the die parting line and the pressure required of the machine to inject metal into the die cavity governs the clamping force of the machine. [1]

Die casting dies have four basic functions.

- Holding molten metal in the shape of the desired casting.
- Provides a mean for molten metal to get to a space where it will be held to the desired shape.
- Remove heat from the molten metal to allow the metal to solidify.
- To provide means for removal of casting.

*Single cavity to produce one component*

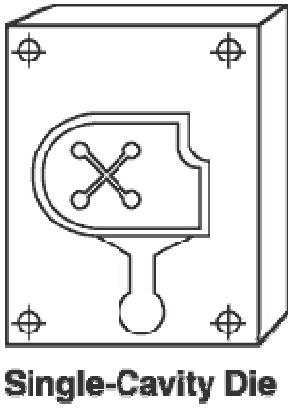


Figure 1.3: Single-cavity die [1]

*Multiple cavities to produce a number of identical parts*

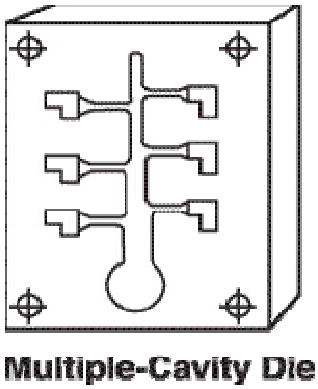


Figure 1.4: Multiple-cavity die [1]

*Unit dies to produce different parts at one time*

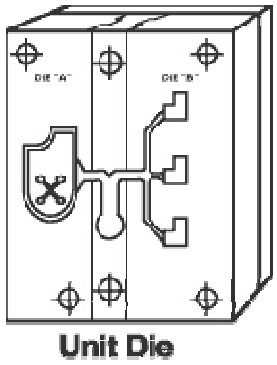


Figure 1.5: Unit die [1]

*Combination dies to produce several different parts for an assembly.*

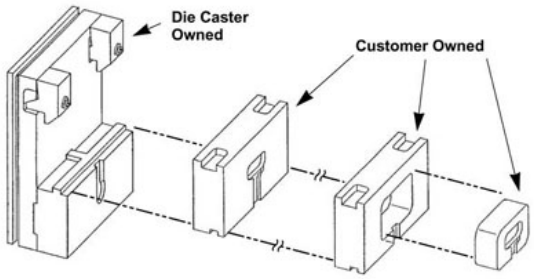


Figure 1.6: Combination dies [1]

Die are generally of moveable and stationary type.

In a simple two part die cavities may be created in the fixed member (the whole of impression in fixed platen) or whole of the impression in moving platen. The form of the component sometime makes only one of these positions practically. But in general the die designer must choose that which offers the best product, well finished and at fastest rate.

It is essential that casting shall be retained by ejector half of the die during the opening stroke, and this is the best achieved by making the impression in such a way that the solidified metal tend to deposit on the ejector die and away from the opposite fixed die member.

### 1.5.1 Die Coating

The function of the die coating is to provide a layer deposited on the walls to control the different condition of metal alloy and for its solidification and to facilitate release of the casting & prolong die life, etc.

The principal functions required of a coating for die casting are:

- Control of the metal flow to ensure that it reaches all parts of the die at a sufficient temperature to prevent the formation of seams, cold laps, etc.
- Control of heat transfer to obtain better solidification and ensure that the castings are properly fed.
- Easy release: since castings are extracted at just below the solidification temperature, easy release ensures that castings do not come out deformed.
- Good surfaces, and therefore a reduction in finishing costs. Longer die life, therefore increased productivity and reduced maintenance.

These results are directly in line with the characteristics of DYCOTE.

(*FOSECO, the Logo and DYCOTE are Trade Marks of the Foseco Group of Companies, used under licence).*

### 1.5.2 Coating Application Method

The coating can be applied using several methods:

- Brush
- Spray
- Immersion

For dies the quickest and most suitable method is spray application. Brush application is reserved for plain areas, or for small details that must be coated in a different way from the rest of the die. Immersion application is mainly used for copper alloys, where the coating also has to cool the die. [5]

### 1.5.3 Die Paint

Die paint is applied to the pouring basin which provide insulation to the pouring basin. Usually die paint is a combination of calcium silicate (5% to 10%), bentonite (5% to 7%), rest of the material is tracoat.

### 1.5.4 Spoon Paint

Spoon paint is also applied in the laddel to avoid sticking of metal and it also helps to retain the temperature.

### 1.5.5 Die Temperature

Dies generally are preheated to a temperature of around 300 to 400 °C, this can be achieved by repeating the trial shorts or can be achieved by heating up the dies by some external source.

### 1.5.6 Cooling of die

Cooling of the die is necessary (in case of high production) so that temperature of the die may not increase beyond its limit. Moreover cooling with water and/or air decreases its solidification time by taken heat from the molten metal. Cooling may be done on various parts on the die for a particular delay on other parts and cooling time may provide directional solidification. Cooling with water or air is accomplished by air or water solenoid valves. Cooling and delay time is set by providing a timer accordingly to the type of casting.

## 1.6 DIE CASTING ALLOYS

Die casting alloys are normally non-ferrous and there is a large number available with a wide range of physical and mechanical properties covering almost every conceivable application a designer might require. Aluminium and zinc alloys are the most widely used, Followed by magnesium, zinc-aluminum (ZA) alloys, copper, tin and lead. Zinc, lead and tin based alloys are classified as low melting point metals because they turn melt at less than 725°F (385°C). Zinc-aluminum (ZA) alloys have a slightly higher melting range of 800°F to 900°F (426°C to 482°C). Aluminum and magnesium alloys are considered to be moderate melting point alloys, being cast in the 1150°F to 1300°F (621°C to 704°C) range. Copper alloys are considered to be high melting point alloys, over 1650°F (899°C). Low melting point alloys are cast in hot chamber machines. Intermediate and high melting point alloys are cast in cold chamber machines.

### 1.6.1 CHOOSING THE PROPER ALLOY

Each of the metal alloys available for die casting offers particular advantages for the completed part.

***Zinc***

The earlier alloy to cast, it offers high ductility, high impact strength, and easily plated. Zinc is economical for small parts, has low melting point and promotes long die life.

***Aluminum***

Aluminum alloy is light in weight, while processing high dimensional stability for complex shapes and thin walls. Aluminum has good corrosion resistance and mechanical properties, high thermal and electrical conductivity, as well as strength at high temperatures.

***Magnesium***

The earliest alloy to machine, magnesium has an excellent strength to weight ratio and is lightest alloy commonly die cast.

***Copper***

This alloy possesses high hardness, high corrosion resistance, and high mechanical properties of alloy cast. It offers excellent wear resistance and dimensional stability, with strength approaching that of steel parts.

***Lead and Tin***

These alloys offer high density and are capable of producing parts with extremely close dimensions. They are also used for special form of corrosion resistance [1].

Alloys of aluminium are used in die casting more extensively than alloys of any other base metal. The die casting process consumes almost twice as much tonnage of aluminum alloys as all other casting processes combined.

Die casting is especially suited to production of large quantities of relatively small parts. Aluminium die castings weighing up to about 5 kg are common, but castings weighing as much as 50 kg are produced when the high tooling and casting-machine costs are justified.

### 1.6.2 ALUMINUM ALLOYS

Aluminium die casting alloys are lightweight, offer good corrosion resistance, ease of casting, good mechanical properties and dimensional stability. Although a variety of aluminium alloys can be die cast from primary or recycled metal, most designers select a standard alloy. Special alloys for special applications are available but their use usually involves significant cost premiums.

## 1.7 Organization of Study

Whole study has been divided into eight chapters.

Chapter 1: This chapter gives the introduction of cold chamber die casting process. This chapter also includes the brief description of various types of dies, types of metals/alloys that can be used in die casting process. It also includes the advantages of die casting.

Chapter 2: This chapter includes the literature review of die casting process. The total literature has been categorized into four categories. It also includes the gap in literature and problem formulation.

Chapter 3: This chapter gives the description of design of experiment and experimental design of study, the experimental set up, process parameters levels and orthogonal array for experiment.

Chapter 4: This chapter includes the observation table of the responses and also include the analysis of the observed data using ANOVA. It gives us the idea about the significant and non significant input factors. The optimal design is also included in this chapter.

Chapter 5: This chapter includes the MRSN of the observed data. It also includes the regression equation developed after the analysis.

Chapter 6: This chapter includes the different microstructure obtained during the phase transformation.

Chapter 7: This chapter includes all the observation and results obtained in the study.

Chapter 8: This chapter includes results, conclusions and recommendations.

# CHAPTER 2

# LITERATURE REVIEW

## 2.1 INTRODUCTION

A large work has been done on different aspects of cold chamber die casting process. This chapter covers the literature on die casting machine settings and other process parameters. The literature has been categorized into the following sections:

**a)** Interfacial heat transfer

**b)** Effect of cooling

**c)** Effect of pressure

**d)** Micro porosity

**e)** Effect of process parameters

**C.P. Hallam and W.D. Griffiths [8]** measured interfacial heat-transfer coefficients during the solidification of Al-Si alloys against coated die steel chills with varying chill temperature, coating thickness and coating type. Two principal resistances to heat transfer across the casting-chill interface were identified, namely, (1) the resistance to heat transfer of the coating itself and (2) the resistance to heat transfer of a layer of gas, (assumed to be air), trapped between the coating and casting surfaces by virtue of their roughness. These thermal resistances were evaluated by measurement of the coating thermal conductivity and determination of the thickness of the applied coatings and the thickness of the layer of air between the coating and casting surfaces. This produced a simple equation to predict the interfacial heat transfer coefficient during the solidification of Al alloy die castings, which produced values that were found to agree well with the experimentally determined results. This equation was used to interpret the experimentally measured heat-transfer coefficients and to explain their variation with the different experimental conditions employed. A simple modification of the equation can also take into account the formation of an air gap, where the casting locally retreats away from the die surface, leading to a local reduction in the heat-transfer coefficient.

**Guo Zhi-peng et al. [9]** focuses on the determination of the interfacial heat transfer coefficient (IHTC) at the metal–die interface in the high pressure die casting (HPDC) process. Experiment was conducted and a ‘‘step shape” casting was used to cast a magnesium alloy AM50 against a H13 steel die. Based on the temperature measurements inside the die, IHTC was determined by applying an inverse approach. The influences of the step thickness and process parameters on the IHTC were investigated. Results show that the shape of IHTC profiles is different at different steps and the duration for IHTC to maintain a higher value grows as the step thickness increases. The influence of process parameters is mainly on the IHTC peak value. For thinner steps, a higher fast shot velocity leads to a higher IHTC peak value. But for thicker steps such as Step 5, the casting pressure shows a more prominent influence on the IHTC peak value. Also, at these thicker steps a lower initial die surface temperature always leads to a higher IHTC peak value**.**

**PENG et al. [10]** investigated the effects of process parameters, casting thickness, and alloys on the metal-die interfacial heat-transfer coefficient (IHTC) in the HPDC process. Experiment was carried out on a cold-chamber die-casting machine with two casting alloys AM50 and ADC12. A special casting, namely, ‘‘step-shape’’ casting, was used and cast against a H13 steel die. The IHTC was determined using an inverse approach based on the temperature measurements inside the die. Results showed that the IHTC was different at different steps and changes as the solidification of the casting proceeds. Process parameters only influenced the IHTC in its peak value, and for both AM50 and ADC12 alloys. Results also showed that a closer contact between the casting and die could be achieved when the casting alloy is ADC12 instead of AM50, which consequently leads to a higher IHTC.

**Zhipeng et al. [11]** focused on the determination of the interfacial heat transfer coefficient (IHTC) between metal and die during the high pressure die casting (HPDC) process. Experiments were carried out on an aluminum alloy, ADC12Z, using “step shape” casting—so-called because of its shape. The IHTC was successfully determined by solving one of the inverse heat problems using the nonlinear estimation method first used by Beck. The calculation results indicated that the IHTC immediately increased after liquid metal was brought into the cavity by the plunger and decreased as the solidification process of the liquid metal proceeded. The liquid metal eventually solidified completely, a condition when the IHTC tended to be stable. Casting thickness played an important role in affecting the IHTC between the metal and die not only in terms of its value but also in terms of its change

tendency. Also, under the test conditions, different change tendencies of the metal solid fraction were found between castings with different thicknesses and the die.

**Persson et al. [12]** experimentally evaluated the temperature variations in the surface layer of hot work tool steel during actual brass die casting. A special method was developed to measure the temperature in the surface layer of the mould at different depths. Untreated, borided, and physical vapor deposition (PVD) coated (CrN) tools were included. Temperature profiles in the surface layer of the mould were recorded and details of the thermal cycling were obtained. Starting with a tool of room temperature, the tool temperature range averages during the initial 20 casting events. Simultaneously, within a surface layer of about 2mm thickness, the maximum stress is reduced to a constant level. Based on the temperature profiles, the maximum surface temperature of the mould and the thickness of the tool surface layer within which fatigue damage can occur were estimated to about 826 ◦C and 1.5 mm, respectively. This limited thickness results from the decrease in temperature range and, consequently, stress from the tool surface and inwards. Finally, no notable influence of the investigated surface engineering on the thermal conditions was found.

**Micowski Teufert [13]** presented results of an investigation of methods of controlling flash and the applications of a real-time closed-loop shot control system to control impact pressure. The process of making various parts using the high-pressure die casting process was examined using a comprehensive process monitoring system and controlled by a seven-phase real-time closed-loop shot control system. They described requirements and benefits of the low-impact control system.

**Dargusch et al. [14]** determined the effects of process variables on the quality of high-pressure die cast components with the aid of in-cavity pressure sensors. In particular, the effects of set intensification pressure, delay time, and casting velocity have been investigated. The in-cavity pressure sensor has been used to determine how conditions within the die-cavity are related to the process parameters regulated by the die casting Machine, and in turn the effect of variations in these parameters on the integrity of the final part. Porosity was found to decrease with increasing intensification pressure and increase with increasing casting velocity. The delay time before the application of the intensification pressure was not observed to have a significant effect on porosity levels.

**Chiang, Liu & Tsai [15]** proposed mathematical models for the modeling and analysis of the effects of machining parameters on the performance characteristics in the HPDC process of Al–SI alloys which were developed using the response surface methodology (RSM) to explain the influences of three processing parameters (die temperature, injection pressure and cooling time) on the performance characteristics of the mean particle size (MPS) of primary silicon and material hardness (HBN) value. The experiment plan adopts the centered central composite design (CCD). The separable influence of individual machining parameters and the interaction between these parameters were also investigated by using analysis of variance (ANOVA). With the experimental values up to a 95% confidence interval, It was fairly well for the experimental results to present the mathematical models of both the mean particle size of primary silicon and its hardness value. Two main significant factors involved in the mean particle size of primary silicon were the die temperature and the cooling time. The injection pressure and die temperature also have statistically significant effect on microstructure and hardness.

**Jerald Brevick et al [16]** conducted a literature review regarding energy used in die-casting, and then create and distribute a survey regarding energy consumption to North American Die Casting Association (NADCA) corporate members. The survey responses were then collected and evaluated. The goal of these activities was to establish an accurate flow chart capable of mapping energy inputs for the die-casting industry. Also, these data were used to determine the relative importance of various energy consuming operations in die-casting, and to determine the amount and quality of energy data available in the industry. In addition to energy survey data, selected energy audits of die-casting operations at the, The Ohio State University (OSU) die-casting laboratory and at industry sites were conducted. The purpose of these audits was to establish the relative amount of energy required by various die-casting operations, such as alloy melting, alloy holding, and the die-casting operation itself. Based on the information derived from the energy survey and on-site energy audits, computer-based models were developed that allow the energy "journey" in die-casting operations to be assessed.

**Patrzalek et al. [17]** investigated feedback and modelling on high pressure die casting processes to investigate them as a whole. The research is specifically aimed at high pressure die casting processes but analogous processes (such as injection molding and thixomoulding) that used cooling channels to stabilize or balance die temperature profiles could also benefit

from this research. A key element of this research program was the development and construction of a small, prototype casting system that could be used to explore the validity of any developed, thermal models.

***H. Yamagataa*** **et al [18]** investigated the effect of average cooling rates on the microstructure of the hypereutectic Al–20% Si alloy, using the novel Universal Metallurgical Simulator and Analyzer Platform. The quantitative measurements of the primary Si size and the Secondary Dendrite Arm Spacing of the non-equilibrium -aluminum as a function of the cooling rates was performed for the laboratory test samples. This research was carried out in order to analyze the microstructure of the high pressure die cast cylinder block and to understand its complex solidification process. The Equivalent Diameter of the primary Si decreased from 89.7±17.3 to 16.5±3.8m and the Secondary Dendrite Arm Spacing from 22.1±5.9 to 5.1±0.8m with an increase in the cooling rate from 4.9 to 82.9 ◦C/s. Observations of the cylinder block microstructures revealed that the primary Si size was nearly identical at the subsurface and the centre locations of the bore wall. The Secondary Dendrite Arm Spacing of the no equilibrium -aluminum phase as well as the eutectic Si size was significantly smaller at the subsurface of the bore wall. Based on the UMSA laboratory measurements it was determined that the primary Si in the engine bore wall (both at the subsurface and the centre) nucleated as a first phase from the liquid melt at a cooling rate of approximately 72–74 ◦C/s. It was found that the non-equilibrium -aluminum dendrites at the engine bore wall subsurface nucleated from the semi-solid melt at a cooling rate of approximately 85 ◦C/s, while at the centre of the bore wall at approximately 49 ◦C/s. Research revealed that some primary Si particles nucleated from the beginning of the melt pouring into the shot sleeve prior to the injection process while the -aluminum dendrites and eutectic Si nucleated in the die cavity. Therefore, it was proven that the injected hypereutectic Al–20% Si liquid melt had solid primary Si particles.

**Horacio Ahuett-Garza** and **R. Allen Miller** [19] determined the quality of a die cast product to a great extent by the mechanism of cavity fill. The evolution of this process has received attention both in industry and literature. Because of its effect on the cost of a numerical simulation, the question of whether or not the filling stage takes place under isothermal conditions needs to be addressed. They analyzes the process of fill in die casting and presents relations that can be used to predict those conditions under which heat release may be

significant. They also introduced and discussed the effects of heat released during fill on the prediction of die casting die deflections

**Q. HAN and S. VISWANATHAN** [20] proposed a mechanism of soldering of an aluminum alloy die casting to a steel die. A soldering critical temperature was postulated, at which iron begins to react with aluminum to form an aluminum rich liquid phase and solid intermetallic compounds. The critical temperature was used to predict the onset of die soldering, and the local liquid fraction is related to the soldering tendency. Experiments have been carried out to validate the concept and to determine the critical temperature for die soldering in an iron-aluminum system. They used thermodynamic calculations to determine the critical temperature and soldering tendency for the cases of pure aluminum and a 380 alloy in a steel mold. They discussed factors affecting the soldering tendency and also suggested methods for reducing die soldering.

**Sumanth Shankar and Diran Apelian [21]** provided a comprehensive understanding of the reactions at the ferrous die/molten metal interface in a metal mold casting operation. The studies had shown that several important factors influence reactions at the ferrous die/molten aluminum interface, including temperature of the melt, temperature of the die, alloy chemistry of the melt and die, die surface engineering, topographical features, and coatings. They also discussed the effect of the more critical factors on soldering, based on the authors' investigations. In addition, based on a mechanistic understanding of the interface reactions between ferrous die and molten aluminum, recommendations are given for specific processing issues to alleviate soldering during die casting of aluminum alloys.

**Hangai and Utsunomiya [22]** fabricated a closed-cell porous aluminum using gases intrinsically contained in aluminum alloy die castings without using a blowing agent. By incorporating the friction stir processing technique, porous aluminum with a porosity of more than 50 pct was successfully obtained at a holding temperature of 923 to 948 K and a holding time of 10 minutes. This proposed die-casting route has high potential for fabricating porous aluminum at a low cost by a higher productivity process.

**Sabau and Viswanathan[23]** developed a comprehensive methodology that takes into account solidification, shrinkage-driven interdendritic fluid flow, hydrogen precipitation, and porosity evolution for the prediction of the micro porosity fraction and distribution in aluminum alloy castings. The approach may be used to determine the extent of gas and

shrinkage porosity, *i.e.*, the resultant micro porosity which occurs due to gas precipitation and that which occurs when solidification shrinkage cannot be compensated for by the interdendritic fluid flow. The results showed that the effect of micro porosity on the interdendritic fluid flow cannot be neglected. The predictions of porosity profiles were validated by comparison with independent experimental measurements by other researchers on aluminum A356 alloy test castings designed to capture a variety of solidification conditions. The numerical results reproduce the characteristic micro porosity profiles observed in the experimental results and also agree quantitatively with the experimentally measured porosity levels. The approach provides an enhanced capability for the design of structural castings.

**ZHU et al. [24]** developed a numerical model for predicting micro porosity formation in aluminum castings, which describes the redistribution of hydrogen between solid and liquid phases, the transport of hydrogen in liquid by diffusion, and Darcy flow in the mushy zone. One of the key features of the model is that it uses a two-stage approach for porosity prediction. In the first stage, the volume fraction of porosity is calculated based on the reduced pressure, whereas, in the second stage, at fractions solid greater than the liquid encapsulation point, the fraction porosity is calculated based on the volume of liquid trapped within the continuous solid network, which is estimated using a correlation based on the Niyama parameter. The porosity model is used in conjunction with a thermal model solved using the commercial finite-element package ABAQUS. The parameters influencing the formation of micro porosity are discussed including a means to describe the super saturation of hydrogen necessary for pore nucleation. The model has been applied to examine the evolution of porosity in a series of experimental samples cast using unmodified A356 in which the initial hydrogen content was varied from 0.048 to 0.137 (cc/100 g). A comparison between the model predictions and the experimental measurements indicates good agreement in terms of the variation in porosity with distance from the chill and the variation resulting from initial hydrogen content.

**Zhua et al. [25]** studied the die surface states and chemical element distribution of the soldering region in a failed die from a die casting plant. The results showed that there exist numerous micro holes, micro cavities and cracks on the die surface of the soldering region. The diameter of the smaller micro holes was about 0.6 mm and that of the bigger micro holes was more than 15 mm. According to the aluminum distribution on the cross-section of die

soldering region, the mechanisms causing die soldering were being discussed and the soldering was classified as physicochemical, mechanical and mixed soldering. Based on the theoretical models proposed, the effects of process parameters, including temperature and the chemistry of the die and the aluminum casting alloy, the injection pressure and the die surface state, on soldering phenomena have been studied. In addition, they also discussed the formation and spread of soldering to a given die in the die casting process.

**Sevik et al.[26]** produced metal–matrix composites of an aluminum–silicon based alloy (LM6) and $Al_2O_3$ particles with volume fractions of 0.05, 0.10 and 0.15 and in size of 44, 85 and 125 lm using pressure die-casting technique. Density, hardness, tensile strength and wear properties were examined. The density values of the composites increased by adding $Al_2O_3$ particle. The hardness of the composites increased with increasing particle volume fraction and with decreasing particle size. The tensile strength of the composites decreased with increasing particle volume fractions and size. The wear rate of the composites decreased with increasing particle volume fraction and with decreasing particle size but increased proportionally to the applied load. Wear mechanism for the surface of the un reinforced alloy was plastic deformation, whereas for the composites it was the layer deformation on the surface of the composites.

**Kimuraa et al.[27]** investigated the influence of the abnormal structure, such as coarse a phase, scattered chill structure or cold shut, in Japanese Industrial Standard (JIS) AC4CH (Al–7.3%Si–0.3%Mg) aluminum alloy squeeze castings on the reliability of mechanical properties. The shot time lag (STL) and the heat transfer coefficient between molten alloy and shot sleeve were changed as the process parameters to control the formation of the abnormal structure. Two types of sleeve lubricants, conventional oil-soluble lubricant and new-developed high insulating powder lubricant were used to control the heat transfer coefficient. Both the tensile strength and its reliability were remarkably improved by using the powder lubricant or by decreasing the STL.

Regarding the fracture elongation, the average elongation was improved due to the reduction of abnormal structure on the fracture surface. However, the reliability of the fracture elongation was sufficiently improved by neither STL nor the type of lubricants. It was found that the reduction of abnormal structure is effective to improve the strength and fracture elongation of squeeze castings.

**Ying-hui Wei et al [28]** investigated microstructures and properties of die casting components with various thicknesses made of AZ91D alloy by means of scanning electron microscope (SEM), transmission electron microscope (TEM), high-resolution transmission electron microscope (HRTEM), etc. It was concluded that mechanical properties of the die casting components mainly depend on grain size of -Mg phase. At the same time, however, the voids formed by entrapping air during die casting process have a remarkable detrimental effect on the mechanical properties. The compounds have no obvious effect on the mechanical properties even though there was possibility of volume change present to form other compounds in the course of the components' being used.

**Yoshihiko and Soichiro [29]** identified the cause of porosity and to take corrective action in the die-casting process accurately and rapidly, a quantitative estimation of the morphology of pores can be an effective technique. In this study, fractal analysis is proposed to characterize porosity quantitatively in terms of the spatial distribution of a number of pores appearing in a target region. The purpose of the present investigation was to evaluate the proposed fractal analysis by comparing the porosity in two types of aluminum alloy die castings manufactured by different die-casting processes, and to confirm that fractal analysis of the spatial distribution of pores can quantitatively characterize the porosity.

***Kimuraa* et al. [30]** used Al–4.5wt%Mg (JIS AC7A, AA 514) aluminum alloy as a representative non-heat treatment type alloy to examine the effect of the addition of silicon and grain refiner on the reduction of the susceptibility to cracking.

In order to evaluate the susceptibility to cracking, both the "I-beam casting cracking test" and the "TIG spot welding cracking test" were carried out. As a result, the addition of Ti + B worked as a grain refiner on both testing methods. The susceptibility to cracking was significantly reduced by the addition of Ti + B in both the I-beam casting and the weld crater. It was found that the finer grain size led to lower susceptibility to cracking. Furthermore, the susceptibility to cracking of the die casting product decreased with the addition of Ti + B.

**Hong and Suryanarayana [31]** studied the effect of powder particle size on the microstructure, mechanical properties, and fracture behavior of Al-20 wt pct Si alloy powders in both the gas-atomized and extruded conditions. The microstructure of the as-atomized powders consisted of fine Si particles and that of the extruded bars showed a homogeneous distribution of fine eutectic Si and primary Si particles embedded in the Al matrix. The grain

size of FCC-Al varied from 150 to 600 nm and the size of the eutectic Si and primary Si was about 100 to 200 nm in the extruded bars. The room-temperature tensile strength of the alloy with a powder size 26 m was 322 MPa, while for the coarser powder (45 to 106 m), it was 230 MPa. The tensile strength of the extruded bar from the fine powder (26 m) was also higher than that of the Al-20 wt pct Si-3 wt pct Fe (powder size: 60 to 120 m) alloys. With decreasing powder size from 45 to 106 m to 26 m, the specific wear of all the alloys decreased significantly at all sliding speeds due to the higher strength achieved by ultra fine-grained constituent phases. The thickness of the deformed layer of the alloy from the coarse powder (10 m at 3.5 m/s) was larger on the worn surface in comparison to the bars from the fine powders (5 m at 3.5 m/s), attributed to the lower strength of the bars with coarse powders.

**BLUM et al. [32]** described the creep of die-cast Mg alloys as an integral part of their plastic deformation behavior in terms of stress-strain–rate-strain relations. Creep tests yield information on yield stress, work hardening, maximum deformation resistance (minimum creep rate), and work softening. Testing in compression avoids influences by fracture. Data on the alloy AJ52 (5Al, 2Sr) in the temperature range between 135 °C and 190 °C are presented and compared to those for AZ91 and AS21. Die-cast Mg-Al alloys consist of fine grains with a grain boundary region containing inter metallic precipitates. Transmission electron microscopic observations indicate that basal glide is the dominant mechanism of deformation being supplemented by non basal glide and twinning to maintain compatibility between the grains. The deformation resistance can be modeled with a composite approach assuming that the grain boundary region is relatively hard due to precipitation of inter metallic phases. The differences in long-term creep resistance at low stress are explained in terms of different strength and stability of precipitates in the different alloys.

Die casting alloys are normally non-ferrous and there is a large number available with a wide range of physical and mechanical properties covering almost every conceivable application a designer might require. Aluminium and zinc alloys are the most widely used, followed by magnesium, zinc-aluminium (ZA) alloys, copper, tin and lead. Zinc, lead and tin based alloys are classified as low melting point metals because they turn melt at less than 725°F (385°C). Zinc-aluminium (ZA) alloys have a slightly higher melting range of 800°F to 900°F (426°C to 482°C). Aluminium and magnesium alloys are considered to be moderate melting point alloys, being cast in the 1150°F to 1300°F (621°C to 704°C) range. Copper alloys are

considered to be high melting point alloys, Over 1650°F,(899°C). Low melting point alloys are cast in hot chamber machines. Intermediate and high melting point alloys are cast in cold chamber machines [33].

The primary function of the die lubricant is to provide a thin film on the surface of the die that will provide a barrier between the molten metal and the die & thus prevent soldering. It also acts as a release agent that facilitates easy ejection of casting from the die and also helps in cooling the die [34].

## 2.2 GAP IN LITERATURE

After studying the literature it can be concluded that a lot of work has been done in the field of high pressure cold chamber die casting process in one way or another. Some investigators [8], [9], [10], [11], have studied the interfacial heat transfer between metal and die during high pressure die casting. Some other researchers [17], [18], [19] investigated the effect of control of cooling, the average cooling rate and the effect of heat released. Some studied [13], [14] the control of impact pressure and the influence of pressure during solidification. A few [23], [24] have predicted micro porosity and modelling of micro porosity and the others [20], [21], [25] studied the preventive measure of die soldering during aluminium die casting, and very few [14], analysis the effect of process parameter on the performance characteristics in high pressure die casting process.

After observing the literature available regarding the high pressure die casting, the literature reveal that a lot of work has been done on interfacial heat transfer, micro porosity die soldering, and to optimize the process parameter but very little work has been reported on input factors that have combine effect on die cast product. No work has been reported in literature which explains the multi response optimisation of the cold chamber die casting process parameters. Moreover, no work has been reported in literature which optimises the cold chamber die casting process parameters using LM6 aluminium alloy. LM6 aluminium alloy has very wide number of applications in automobile industry but still not much work is available on its properties with different input process parameters.

## 2.3 PROBLEM FORMULATION

Based on the literature survey and the subsequent analysis of gaps the present work aims to investigate the effect of various parameters in a die casting process on the properties of

aluminium alloy and optimize the parameters using multi-response optimization methodology. The experiments have been conducted using aluminium alloys LM 6. The process parameters varied were the thermal characteristics (temperature of the molten metal), the injection pressure of molten metal, Coating thickness and solidification rate. The properties and quality of die cast components are directly related to the microstructure of die cast component. This research study has been carried out on the existing die casting machine in the workshop.

## 2.4 OBJECTIVES

- To evaluate the effect of process parameter (pouring temperature, injection pressure, coating thickness and solidification rate) on the properties of the cast metal.
- To evaluate the significant interactions between the above factors.
- To analyze the machined surface for microstructure and hardness to study the change in material properties as a result of the experimentation.
- To develop a linear empirical model.

This has been done by factorial analysis of variance. The factor analysis parameterization approach has been used to study the effect of various factors at appropriate levels. Multiple regression models have been used to determine the best-fit relationship between the response and the model parameter. After studying the effect of parameters using a parametric approach a study on material properties and effect of process parameters has been completed.

## 2.5 WORK PLAN

Following activity have been carried out to complete the project

1. Preparatory work
   (a) Selection of die casting alloy.
   (b) Procurement of material to make the required alloy and preparation of samples.
   (c) The samples will be machined on the grinding machine at TU, Patiala.
2. After finalization of the significant process parameters detailed experiments were carried out with all possible variations, included in the study.
3. Measurements were taken for each process variable and results were analyzed using ANOVA to arrive at a method which satisfies the requirement of the cast product.

4. Study of material properties.
5. Multi response optimisation was done using MRSN technique

# CHAPTER 3

# EXPERIMENTAL DESIGN

## 3.1 INTRODUCTION

Die casting is a versatile process for producing engineered material/metal parts by forcing molten metal under high pressure into reusable die steel moulds. These moulds called dies can be designed to produce complex shapes with high degree of accuracy and repeatability. Parts can be sharply defined with smooth or textured surface and are suitable for a wide variety of attractive and serviceable finishes. The effect of various process parameters was studied after the machining of die cast parts. Different Parameters (viz. temperature of the molten metal, injection pressure of the molten metal, type of coating, and the type of cooling) was studied using parameterization approach developed by Taguchi [35].

The full factorial design is referred as the technique of defining and investigating all possible conditions in an experiment involving multiple factors while the fractional factorial design investigates only a fraction of all the combinations. Although these approaches are widely used, they have certain limitations: they are inefficient in time and cost when the number of the variables is large; they require strict mathematical treatment in the design of the experiment and in the analysis of results; the same experiment may have different designs thus produce different results; further, determination of contribution of each factors is normally not permitted in this kind of design. The Taguchi method has been proposed to overcome these limitations by simplifying and standardizing the fractional factorial design. The methodology involves identification of controllable and uncontrollable parameters and the establishment of a series of experiments to find out the optimum combination of the parameters which has greatest influence on the performance and the least variation from the target of the design [36].

## 3.2 ESTABLISHMENT OF OBJECTIVE FUNCTION

The objective of the study is to evaluate the main effects i.e. thermal characteristics (temperature of the molten metal), injection pressure of the molten metal, type of coating (oil

coating, oil + graphite coating, dycot coating), and the type of cooling (air cooling, water cooling and oil cooling) on work piece material, density of the material, hardness of the material and the surface roughness of the material.

## 3.3 SELECTION OF FACTORS

The determination of which factors to investigate depends on the responses of interest. The factors that are believed to affect the responses were identified using cause and effect analysis, and brainstorming. The lists of factors studied with their levels are given in the Table 3.1

**Table 3.1: Factors of interest and their respective levels**

| FACTOR | Level-1 | Level-2 | Level-3 |
|---|---|---|---|
| Pouring temperature of the molten metal (A) | $750^{0}$ | $770^{0}$ | $790^{0}$ |
| Injection pressure of the molten metal $kg/cm^2$ (B) | 170 | 180 | 190 |
| Type of coating (C) | Oil coating | Oil + Graphite Coating | Dycot coating |
| Type of cooling (D) | Air cooling | Water cooling | Oil cooling |

## 3.4 DEGREE OF FREEDOM (dof)

The number of factors and their interactions and level for factors determine the total degree of freedom required for the entire experimentation. Table 3.2 gives the degrees of freedom of each factor along with total degrees for the freedom of experiment. The degree of freedom for each factor is given by the number of levels minus one.

*dof for each factor : k-1*

Where k is the number of level for each factor

**Table 3.2: Degree of freedom**

| Factor | A | B | C | D | Total |
|---|---|---|---|---|---|
| Degree of Freedom | 2 | 2 | 2 | 2 | 8 |

## 3.5 ORTHOGONAL ARRAY

OA plays a critical part in achieving the high efficiency of the Taguchi method. OA is derived from factorial design of experiment by a series of very sophisticated mathematical algorithms including combinatorics, finite fields, geometry and error- correcting codes. The algorithms ensure that the OA to be constructed in a statistically independent manner that each level has an equal number of occurrences within each column; and for each level within one column, each level within any other column will occure an equal number of times as well. Then, the columns are called orthogonal to each other. OAs is available with a variety of factors and levels in the Taguchi method. Since each column is orthogonal to the others, if the results associated with one level of a specific factor are much different at another level, it is because changing that factor from one level to the next has strong impact on the quality characteristic being measured.

The selection of orthogonal array depends on:

- The number of factors and interactions of interest
- The number of levels for the factors of interest

Taguchi's orthogonal arrays are experimental designs that usually require only a fraction of the full factorial combinations. The arrays are designed to handle as many factors as possible in a certain number of runs compared to those dictated by full factorial design. The columns of the arrays are balanced and orthogonal. This means that in each pair of columns, all factor combinations occur same number of times. Orthogonal designs allow estimating the effect of each factor on the response independently of all other factors. Once the degrees of freedom are known, the next step, selecting the orthogonal array (OA) is easy. The number of treatment conditions is equal to the number of rows in the orthogonal array and it must be equal to or greater than the degrees of freedom. Once the appropriate orthogonal array has been selected, the factors can be assigned to the various columns.

To select an appropriate orthogonal array for experiments, the total degrees of freedom must be computed. The degrees of freedom are defined as the number of comparisons between process parameters that must be made to determine which level is better and, specifically, how much better it is. For example, a two-level process parameter counts for one degree of freedom. The degrees of freedom associated with interaction between two process parameters are given by the product of the degrees of freedom for the two process parameters. In the present study, the interaction between the die casting parameters is neglected. Therefore, there are eight degrees of freedom owing to the four sets of input parameters in the cold chamber die casting process. Once the degrees of freedom are known, the next step is to select an appropriate orthogonal array to fit the specific task. The degrees of freedom for the orthogonal array should be greater than, or at least equal to, those for the process parameters. In this study, an L9 orthogonal array with five columns and nine rows was used. This array has eight degrees of freedom and it can handle four process parameters. Each die casting parameter was assigned to a column and nine die casting parameter combinations were tested. Therefore, only nine experiments are required to study the entire casting parameter space using the L9orthogonal array. The experimental layout for the casting parameters using the L9 orthogonal array is shown in Table 3.3.

**Table 3.3: Orthogonal Array L9**

| Trial No. | Pouring temp. $^0$C | Injection pressure kg/cm$^2$ | Coating type | Cooling Medium |
|---|---|---|---|---|
| 1 | 750 | 170 | Oil Coating | Air Cooling |
| 2 | 750 | 180 | Oil+ graphite | Water Coolig |
| 3 | 750 | 190 | Dycot | Oil Cooling |
| 4 | 770 | 170 | Oil+ graphite | Oil Cooling |
| 5 | 770 | 180 | Dycot | Air Cooling |
| 6 | 770 | 190 | Oil Coating | Water Coolig |
| 7 | 790 | 170 | Dycot | Water Coolig |
| 8 | 790 | 180 | Oil Coating | Oil Cooling |
| 9 | 790 | 190 | Oil+ graphite | Air Cooling |

### 3.6 DESCRIPTION OF DIE CASTING MACHINE

The experiments have been conducted on Horizontal Cold Chamber Pressure Die Casting Machine i.e. Technocrats TDC- 80 available at Central Workshop, Thapar University, Patiala. Die casting machine used for the experiments is shown in the Figure 3.1. The main parts of the machine are control box panel, fixed plate, moving plate, back plate, accumulator, injection cylinder, injection rod, ejector system, oil tank, die regulating valve, pressure regulating valve. The injection pressure can be varied through the pressure regulating valve. Control is provided on the machine for die opening time, closing time and the ejector time for the ejection of cast product. The machine can be operated in manual as well as in automatic mode. The main specifications of the machine are given in table 3.3.

**Table 3.4: Specification of Die Casting Machine**

| | |
|---|---|
| Locking force | 80 tones |
| Injection force | 11.5 tons |
| Hydraulic ejection force | 4 tons |
| Die mounting plates | 520 x 520 (mm) |
| Space between tie bars | 330 x 330 (mm) |
| Max. die height | 400 mm |
| Min. die height | 200 mm |
| Tie bar diameter | 60 mm |
| Die opening stroke | 200 mm |
| Injection stroke | 250 mm |
| Ejection stroke | 50 mm |
| Distance between centre and bottom injection | 85 mm |
| Electric motor capacity | 5.5 kw |
| Working pressure | 100/135 kg/cm2 |

| | |
|---|---|
| Hydraulic pump (vane type) | 70 ltr./min |
| Oil tank capacity | 300 ltr. |
| Machine weight | 3.5 tons |
| Shot capacity | 950 gm |

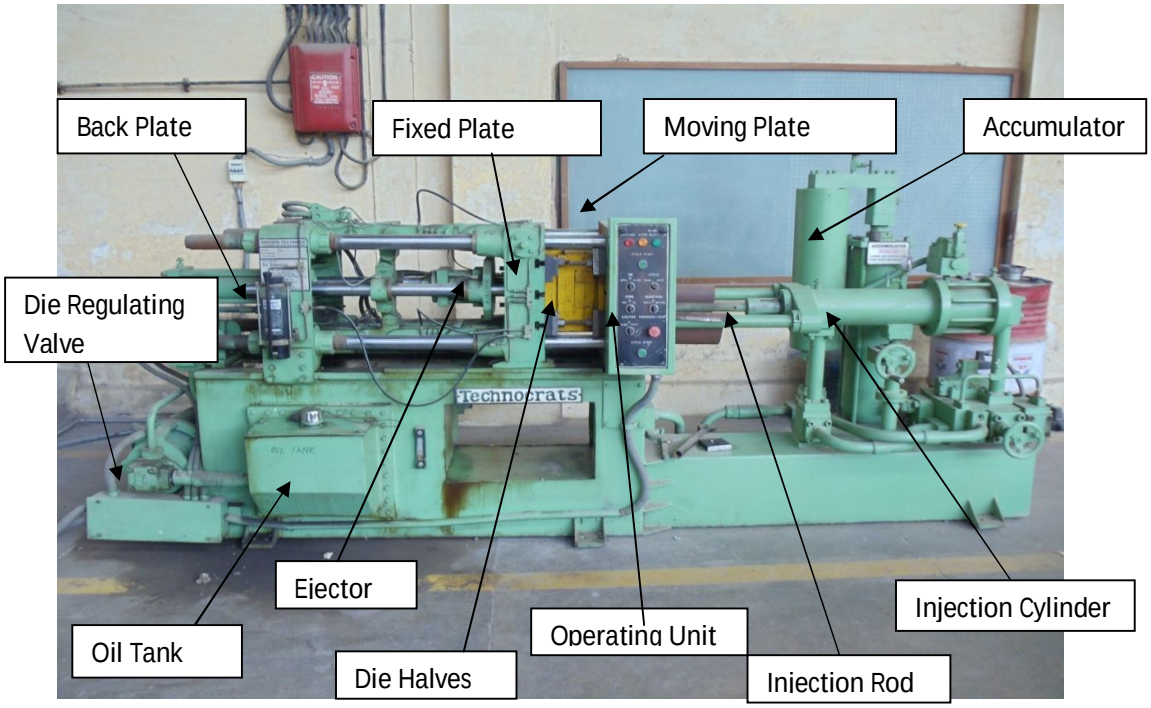


**Figure 3.1 High Pressure Cold Chamber Die Casting Machine at Thapar University**

3.6.1 Operating mode

- Manual Mode: In this mode the machine is not under the casting programme. Direction of operations depends upon the decision of operator.
- Automatic Mode: Machines operations can be programmed e.g. die opening time, die closing time; casting ejection time can be controlled.
- Stop Button: The machine stops when stop button is pushed.

3.6.2 Display indication

- Pressure gauge: the pressure gauges are used to display the pressure of injection of molten metal and to display the pressure of the accumulator.

## 3.7 DESCRIPTION OF MUFFLE FURNACE

The metal was melted in a muffle furnace having maximum temperature range up to $1100^0$ C manufactured by Swastika Engineering and Melting Instruments Ambala, India, available at Central Workshop, Thapar University Patiala. The Muffle furnace used for the experiments is shown in the Figure 3.2. The main part of the machine is casing which accommodates the heating element in between the sheet and the heating chamber with the aid of refractory brick lining, swing door with a peep hole provided on the top of heating chamber. The melting temperature can be varied and controlled by inbuilt pyrometer indicator with energy control. An electrical control panel box houses all the electrical parts that work on 220/240 volts AC single/three phase mains.

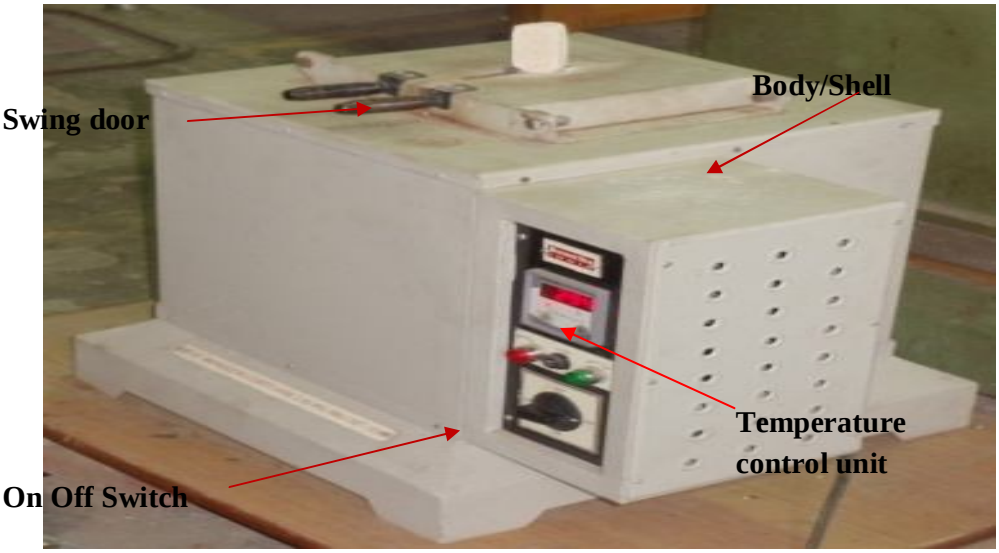


**Figure 3.2: Muffle Furnace**

## 3.8 EXPERIMENTAL SET UP

The machine was operated at standard operating conditions except the injection pressure which was varied at 170,180,190 kg/cm$^2$ as per experimental design. The other factors which were varied as per experimental design are the coating (oil coating, oil + graphite coating and dycot), the cooling medium of the cast product (air cooled, water cooled, oil cooled), the pouring temperature of the molten metal ($750^0$ C, $770^0$ C, $790^0$ C,). The metal was poured in

the injection chamber in the injection sleeve with the aid of pouring spoon. L9 orthogonal was used for conducting the experiments. All the trial conditions using L9 orthogonal array are listed in Table 3.1. The experiments were conducted in the Foundry Section at Central Workshop, Thapar University Patiala.

The muffle furnace was used for melting the LM6 alloy (as described in table 3.6) at different temperature conditions as per experimental design. The temperature was controlled by inbuilt pyrometer indicator with energy control.

3.8.1 Dies for Experiment

Dies used for the casting of clutch plates were made of alloy tool steel in two sections, one was fixed die half and the other was ejector die half, to permit the removal of casting. Sprue hole was in the fixed die that allows the molten metal to enter the die and fill the cavity. The fixed die contain the runner (passage way) and gates (inlet) that route the molten metal to the die cavity. Dies included locking pins to secure the two halves, ejector pins to help remove the cast part. When the die casting machine closes, the two die halves are locked and held together by the machines hydraulic pressure.

## 3.9 MEASURING AND TEST EQUIPMENT USED

Rockwell hardness and surface roughness tests were conducted on all the samples, produced after each of the 9 trials. Also, density was measured using a weighing machine, and micrometer. The details of important test equipment used in experimental study are given below:

### 3.9.1 Surface Roughness Tester

Surface roughness was measured using the Mitutoyo Surftest model SJ-301 available in Metrology laboratory at Baba Banda Singh Engineering College, Fatehgarh Sahib, and Punjab, India. The equipment uses the stylus method of measurement, has profile resolution of 12 nm and measure roughness up to 100μm. A tracing length of 4.8 mm was used for analysis.

### 3.9.2 Rockwell Hardness Tester

Hardness was measured on a Rockwell Hardness Tester, (model AVERY 6402) England, available at Strength of Material Laboratory, Thapar University, Patiala. The hardness measurement is dependent on the diameter of indentation on the samples. The indents formed in the pyramid shaped steel ball indenter were measured on B scale with a minor load of 10 kg for 20 Seconds.

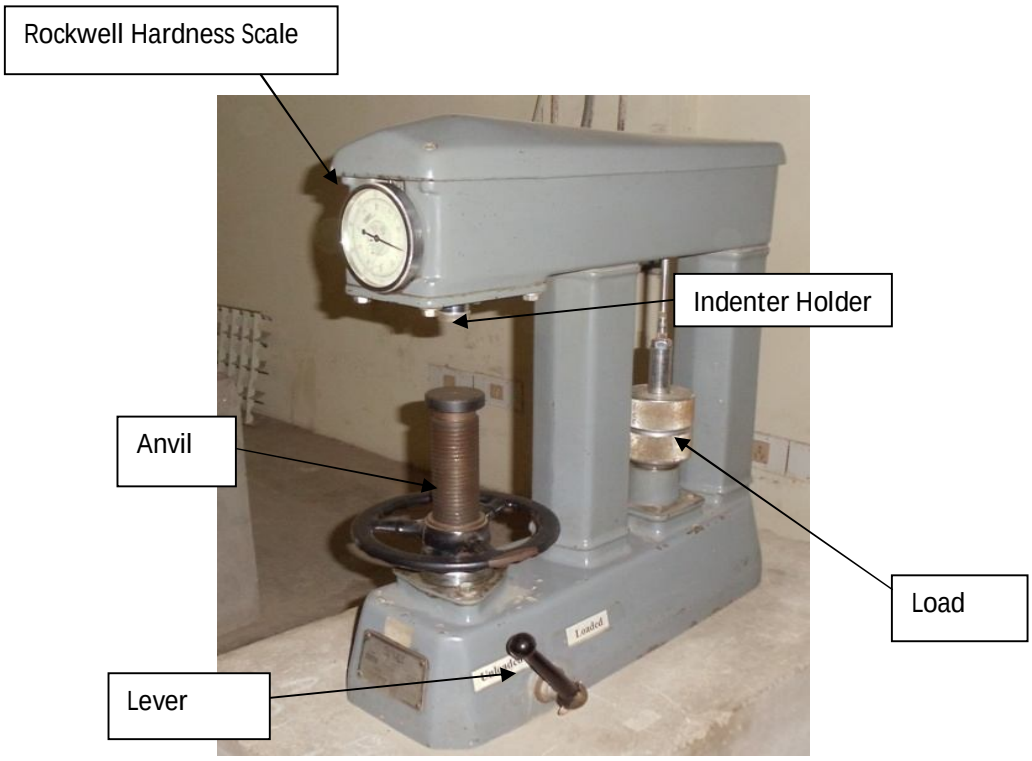


**Figure 3.3: Rockwell Hardness Testing Machine**

### 3.10. COMPOSITION OF WORK MATERIAL

The Aluminium alloy LM6 was used as work piece material. The percentage composition of the work piece material is provided in Table 3.6. The work pieces are shown in the Figure 3.4 and work pieces after casting as a final sample are shown in Figure 3.6.

**Figure 3.4: Raw material of LM-6 before casting**

**Table 3.5: Chemical composition of work piece materials**

| | % composition of aluminium alloy LM6 | | | | | | | | | | | | | |
|---|---|---|---|---|---|---|---|---|---|---|---|---|---|---|
| | Si | Fe | Cu | Mn | Mg | Zn | Cr | Be | Ni | Ti | Pb | Sn | Sr | Sb |
| Value | 12.20 % | 0.420 % | 0.0820% | 0.423 % | 0.0820 % | 0.0620 % | 0.0184 % | 0.0050% | 0.0560 % | 0.152% | 0.0943% | 0.0208% | <0.000010% | 0.00689% |
| | Na | B | Zr | Ga | Co | V | Ca | Ag | Cd | In | Bi | Hg | La | Ba |
| Value | 0.0032 4% | 0.0160 % | 0.0352 % | 0.0640% | <0.00050 % | 0.0743% | <0.00010 % | 0.0030% | <0.00010 | <0.00030 % | <0.00100 % | 0.0232% | <0.000030% | <0.000010% |
| | Ba | P | Ce | Li | Al | | | | | | | | | |
| Value | <0.00010 % | 0.0046 1% | <0.000150% | <0.00010 % | 86.8% | | | | | | | | | |

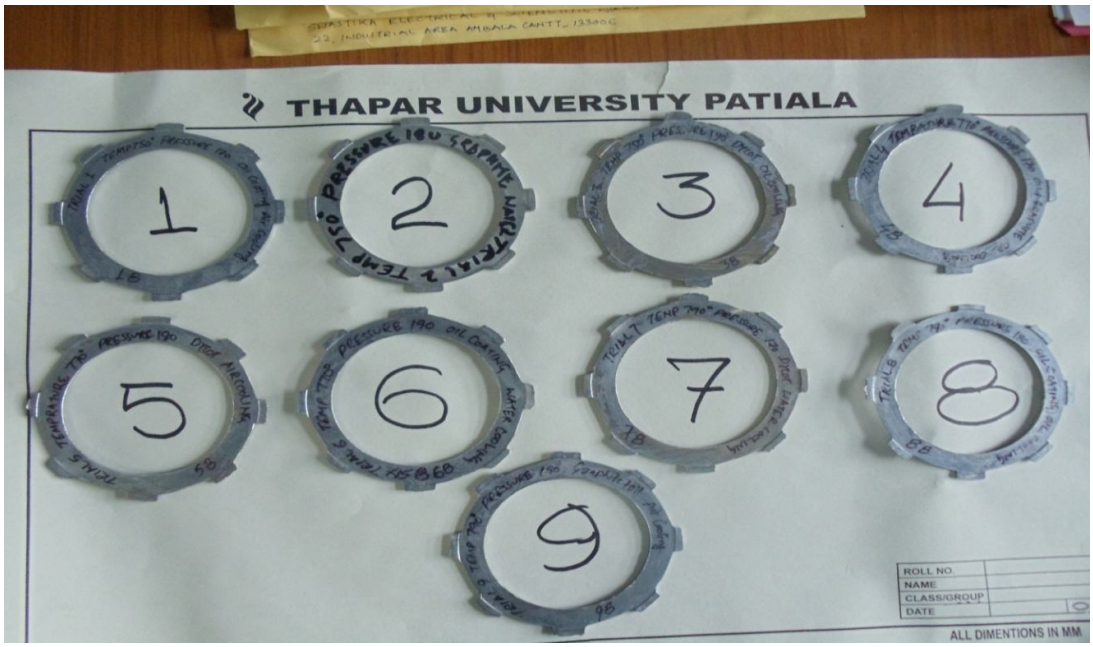


**Figure 3.5: Final Sample of Material of LM-6 after casting**

### 3.11 ANALYSIS OF RESULTS

The results for surface hardness, density and hardness after each of the 9 trials conducted with repetition are given in table: 3.6.

**Table 3.6 Analysis of results**

| Trial No. | Pouring temp. $_0$C | Injection pressure kg/cm$^2$ | Coating type | Cooling type | Surface roughness ($R_a$) | | Mean $R_a$ | Density | | Mean Density | Hardness | | Mean Hardness |
|---|---|---|---|---|---|---|---|---|---|---|---|---|---|
| | | | | | I | II | | I | II | I | I | II | |
| 1 | 750 | 170 | Oil Coating | Air Cooling | 2.22 | 2.16 | 2.22 | 2.30 | 2.30 | 2.30 | 70.00 | 71.66 | 70.83 |
| 2 | 750 | 180 | Oil+ graphite | Water Coolig | 1.60 | 1.59 | 1.60 | 2.54 | 2.54 | 2.54 | 66.62 | 67.33 | 66.97 |
| 3 | 750 | 190 | Dycot | Oil Cooling | 1.32 | 1.29 | 1.32 | 2.65 | 2.56 | 2.61 | 67.33 | 68.66 | 67.99 |

| | | | | | | | | | | | | | |
|---|---|---|---|---|---|---|---|---|---|---|---|---|---|
| 4 | 770 | 170 | Oil+ graphite | Oil Cooling | 2.26 | 2.24 | 2.26 | 2.14 | 2.14 | 2.14 | 67.00 | 69.00 | 68.00 |
| 5 | 770 | 180 | Dycot | Air Cooling | 1.63 | 1.61 | 1.63 | 2.30 | 2.30 | 2.30 | 75.33 | 71.33 | 73.330 |
| 6 | 770 | 190 | Oil Coating | Water Coolig | 0.90 | 0.87 | 0.90 | 2.40 | 2.40 | 2.40 | 72.66 | 71.66 | 72.160 |
| 7 | 790 | 170 | Dycot | Water Coolig | 2.15 | 2.12 | 2.15 | 2.22 | 2.22 | 2.22 | 70.33 | 71.00 | 70.665 |
| 8 | 790 | 180 | Oil Coating | Oil Cooling | 1.75 | 1.72 | 1.75 | 2.58 | 2.59 | 2.58 | 69.33 | 71.00 | 70.165 |
| 9 | 790 | 190 | Oil+ graphite | Air Cooling | 1.52 | 1.55 | 1.52 | 2.65 | 2.65 | 2.65 | 70.66 | 71.66 | 71.160 |

***Analysis of Variance***

The knowledge of the contribution of individual factors is critically important for the control of the each response. The analysis of variance (ANOVA) is a common statistical technique to determine the percent contribution of each factor for results of the experiment. It calculates parameters known as sum of squares (*SS*), pure *SS*, degree of freedom (dof), variance, F-ratio and percentage of each factor. Since the procedure of ANOVA is a very complicated and employs a considerable of statistical formula, only a brief description of is given as following.

The Sum of Squares (SS) is a measure of the deviation of the experimental data from the mean value of the data.

Let '*A*' be a factor under investigation

$$SS_T = \sum_{i=1}^{N} (y_i - \overline{T})^2$$

Where N = Number of response observations, $\overline{T}$ is the mean of all observations $y_i$ is the i, *th* response

Factor Sum of Squares ( $SS_A$ ) - Squared deviations of factor (*A*) averages from overall average

$$SS_A = \left[ \sum_{i=1}^{k_A} \left( \frac{A_i^2}{n_{Ai}} \right) \right] - \frac{T^2}{N} \qquad \text{(Equation 3.1 )}$$

Where

$A_i$ =Average of all obseravtions under $A_i$ level = $A_i / n_{Ai}$

$T$ = sum of all observations

$\overline{T}$ = Average of all observations = $T / N$

$n_{Ai}$ = Number of obsernations under $A_i$ level

Error Sum of Squares ( $SS_e$ ) - Squared deviations of observations from factor (A) averages

$$SS_e = \sum_{j=1}^{k_A} \sum_{i=1}^{n_{Ai}} \left( y_i - \overline{A}_j \right)^2 \qquad \text{(Equation 3.2 )}$$

$$SS_A^{/} = SS_A - (V_e)(v_A) \qquad \text{(Equation 3.3 )}$$

$SS_A^{/}$ is expected sum of squares due to factor A, and the percent contribution to the total variation can be calculated as:

$$P = \frac{SS'_A}{SS_T} \times 100 \qquad \text{(Equation 3.4 )}$$

***Signal-to-Noise Ratio***

The parameters that influence the output can be categorized into two classes, namely controllable (or design) factors and uncontrollable (or noise) factors. Controllable factors are those factors whose values can be set and easily adjusted by the designer.

Uncontrollable factors are the sources of variation often associated with operational environment. The best settings of control factors as they influence the output parameters are determined through experiments. From the analysis point of view, there are three possible categories of the response characteristics explained below.

$r$ is the number of tests in a trial (noise of repetitions regardless of noise levels)

$\sum_{i=1}^{r} y^2{}_i$ = summation of all response values under each trial

*MSD* = Mean square deviation

$y_j$= Observed value of the response characteristic

$y_o$= nominal or target value of the results

The three different response characteristics are given by the following.

***Higher is Better***. The S/N for higher the better is given by:

$(S/N)_{HB} = -10 \log (MSD_{HB})$

Where $MSD_{HB} = \frac{1}{r}\sum_{j=1}^{r}\left(\frac{1}{y_j^{\,2}}\right)$ (Equation 3.5.)

$MSD_{HB}$ = Mean Square Deviation for higher-the-better response.

***Nominal is Better***. The S/N for nominal is better is:

$(S/N)_{NB} = -10 \log (MSD_{NB})$

Where $MSD_{NB} = \frac{1}{r}\sum_{j=1}^{r}\left(y_j - y_0\right)^2$ (Equation 3.6.)

***Lower is Better***. In this design situation, the surface roughness and hardness is the type of ‘‘lower is better’’, which is a logarithmic function based on the mean square deviation (MSD), given by

$$S/N_{LB} = -10\log(MSD) = -10\log[(\frac{1}{r}\sum_{i=1}^{r} y^2{}_i)$$ (Equation 3.7.)

Where $MSD_{LB} = \frac{1}{r}\sum_{j=1}^{r}\left(y_j^{\,2}\right)$

***Signal To Noise Ratio For Response Characteristics***

The parameters that influence the output can be categorized in two categories, controllable factors and uncontrollable factors. The control factors that may contribute to reduced variation can be quickly identified by looking at the amount of variation present in response. The uncontrollable factors are the sources of variation often associated with operational environment. For this experimental work, response characteristics have given in the Table 3.7.

**Table 3.7: Response Characteristics**

| Response name | Response type | Units |
|---|---|---|
| Density | Higher the better | $gm/cm^3$ |
| Hardness | Lower the better | HRB |
| Surface Roughness | Lower the better | Microns |

***Measurement of F-value of Fisher's F ratio***

The principle of the *F* test is that the larger the *F* value for a particular parameter, the greater the effect on the performance characteristic due to the change in that process parameter. *F* value is defined as:

$$F = \frac{MS\ for\ the\ term}{MS\ for\ the\ error\ term} \qquad \text{(Equation 3.8)}$$

Depending on F-value, percentage contribution is calculated of each factor and interaction.

Computation of average performance:

Average performance of a factor at certain level is the influence of the factor at this level on the mean response of the experiments.

# CHAPTER 4

# RESULTS AND ANALYSIS

## 4.1 INTRODUCTION

The effect of various input parameters i.e. thermal characteristics (temperature of the molten metal), injection pressure of the molten metal, type of coating (oil coating, oil + graphite coating, dycot coating), and the type of cooling (air cooling, water cooling and oil cooling ). The three responses were selected for experimentation namely, surface roughness, density, hardness. The experiment was conducted using LM6 aluminium alloy. The assignment of factor was carried out using statistical software MINITAB. All the factors were varied at three levels. The degree of freedom required for the experiment was calculated to be 8, thus orthogonal array that can be used should have degree of freedom (dof) less than or equal to 8. L9, which can accommodate factors with 3-levels, was thus used for conduct of experiments to measure three responses namely the surface roughness, density and hardness. After conducting the 9 trials the mean value for all the above factors are tabulated. For the analysis of result Analysis of Variance (ANOVA) was performed.

## 4.2 RESULTS OF SURFACE ROUGHNESS ($R_a$)

Surface roughness was measured using the Mitutoyo Surftest model SJ-301 available in the Metrology laboratory at Baba Banda Singh Bahadur Engineering College, Fatehgarh Sahib. The result of surface roughness for each of the 9 experiments is given in Table in 4.1.

**Table 4.1: Results for Surface Roughness ($R_a$)**

| Trial No. | Pouring temp. | Injection pressure | Coating type | Cooling type | Surface roughness ($R_a$) | | Mean surface roughness | S/N ratio |
|---|---|---|---|---|---|---|---|---|
| | | | | | I | II | | |
| 1 | $750^0$ | 170 | Oil Coating | Air Cooling | 2.22 | 2.16 | 2.190 | -6.80970 |
| 2 | $750^0$ | 180 | Oil+ graphite | Water Coolig | 1.60 | 1.59 | 1.595 | -4.05526 |
| 3 | $750^0$ | 190 | Dycot | Oil Cooling | 1.32 | 1.29 | 1.305 | -2.31278 |
| 4 | $770^0$ | 170 | Oil+ graphite | Oil Cooling | 2.26 | 2.24 | 2.250 | -7.04374 |

| | | | | | | | | |
|---|---|---|---|---|---|---|---|---|
| 5 | $770^0$ | 180 | Dycot | Air Cooling | 1.63 | 1.61 | 1.620 | -4.19047 |
| 6 | $770^0$ | 190 | Oil Coating | Water Coolig | 0.90 | 0.87 | 0.885 | 1.05989 |
| 7 | $790^0$ | 170 | Dycot | Water Coolig | 2.15 | 2.12 | 2.135 | -6.58817 |
| 8 | $790^0$ | 180 | Oil Coating | Oil Cooling | 1.75 | 1.72 | 1.735 | -4.78631 |
| 9 | $790^0$ | 190 | Oil+ graphite | Air Cooling | 1.52 | 1.55 | 1.535 | -3.72258 |

## 4.3 ANALYSIS OF VARIANCE- SURFACE ROUGHNESS

The results were analyzed using ANOVA for identifying the significant factors affecting the surface roughness. ANOVA results for the mean surface roughness at 95% confidence interval are given in Table 4.2. The variation data for each factor was tested for F value to find significance of each factor. The principle of F-test is that the larger the F values for a particular parameter, the greater the effect of performance characteristics due to the change in that process parameter. ANOVA analysis showed that injection pressure (F value 10.913) was the only factor that significantly affects the surface roughness. All other factors, namely, pouring temperature, coating and cooling were found to be insignificant. Table 4.3 shows the rank of various factors in the term of their relative significance. Pressure had the highest rank, signifying highest contribution to surface roughness and the coating has the lowest rank and was observed to be insignificant in affecting surface roughness. Main effect plot for the mean surface roughness is shown in the Figure 4.1 which shows the variation of surface roughness with the input parameters. As can be seen surface finish improves with the increase in injection pressure.

**Table 4.2: Analysis of Variance for means of surface roughness ($R_a$)**

| Factors | SS | V | MS | F | SS' | % contribution |
|---|---|---|---|---|---|---|
| Pouring Temperature | 0.07044 | 2 | 0.035219 | | | |
| Injection Pressure | 1.36264 | 2 | 0.681319 | 10.91 | 1.127 | 70.57 |
| Coating | 0.05442 | 2 | 0.027211 | | | |
| Cooling | 0.11017 | 2 | 0.055086 | | | |
| Total | 1.59767 | 8 | | | | |
| E pooled | 0.23503 | 6 | 0.117516 | | | |

**Table 4.3: Response Table for Mean surface roughness ($R_a$)**

| Level | Temperature | Pressure | Coating | Cooling |
|---|---|---|---|---|
| 1 | 1.697 | 2.192 | 1.603 | 1.782 |
| 2 | 1.585 | 1.650 | 1.793 | 1.538 |
| 3 | 1.802 | 1.242 | 1.687 | 1.763 |
| Delta | 0.217 | 0.950 | 0.190 | 0.243 |
| Rank | 3 | 1 | 4 | 2 |

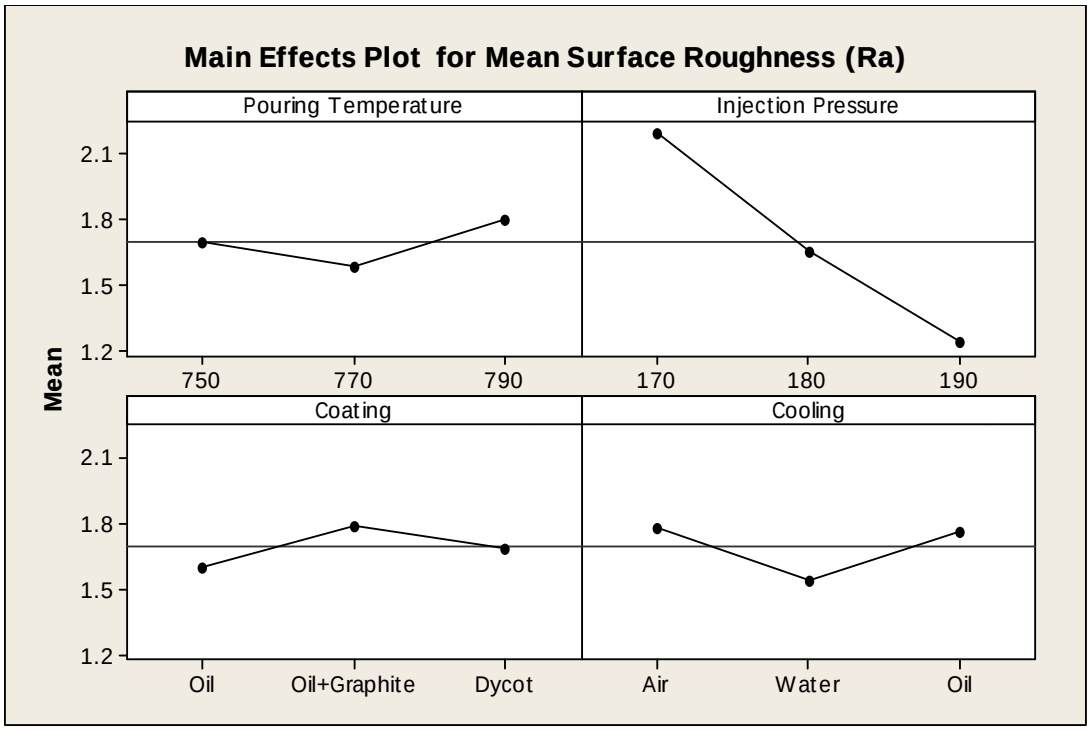


**Figure 4.1: Main effect plot for surface roughness**

## 4.4 RESULTS FOR S/N RATIO – SURFACE ROUGHNESS

The S/N ratio consolidated several repetitions into one value and is an indication of the amount of variation present in the process. The S/N ratios have been calculated to identify the major contributing factors and interactions that cause variation in surface roughness. Surface roughness is a "lower the better" type response and is given by a logarithmic function based on the mean square deviation (MSD),

$$S / N_{LB} = -10 \log( MSD ) = -10 \log[( \frac{1}{r} \sum_{i=1}^{r} y^2{}_i )$$

Where $MSD_{LB} = \frac{1}{r} \sum_{j=1}^{r} \left( y_j{}^2 \right)$

The S/N ratio values are given in the last column of Table 4.1. Table 4.4 shows the ANOVA results for S/N ratio of surface roughness at 95% confidence interval. Other than coating, all other factors, namely, pressure temperature, injection pressure and cooling were found to be significant in affecting surface roughness ($R_a$). According to F-test, injection pressure was observed to be the most significant factor affecting the surface roughness, followed by cooling and pouring temperature according to F-test. Main effect plot of S/N ratio for surface roughness are shown in the Figure 4.2.

**Table 4.4: Analysis of Variance for S/N ratios of surface roughness**

| Source | SS | DOF | MS | F | SS | % contribution |
|---|---|---|---|---|---|---|
| Pouring Temperature | 4.1042 | 2 | 2.0521 | 1.324 | 1.0056 | 1.92 |
| Injection Pressure | 39.8901 | 2 | 19.9450 | 12.873 | 36.79 | 70.24 |
| Coating | 3.0987 | 2 | 1.5493 | | | |
| Cooling | 5.2817 | 2 | 2.6408 | 1.704 | 2.18 | 4.16 |
| e-pooled | 3.0987 | 2 | 1.5493 | | | |
| Total | 52.3746 | 8 | | | | |

**Table 4.5: Response Table for S/N Ratio of Surface Roughness**

| Level | Temperature | Pressure | Coating | Cooling |
|---|---|---|---|---|
| 1 | -4.393 | -6.814 | -3.512 | -4.908 |
| 2 | -3.391 | -4.344 | -4.941 | -3.195 |
| 3 | -5.032 | -1.658 | -4.364 | -4.714 |
| Delta | 1.641 | 5.155 | 1.428 | 1.713 |
| Rank | 3 | 1 | 4 | 2 |

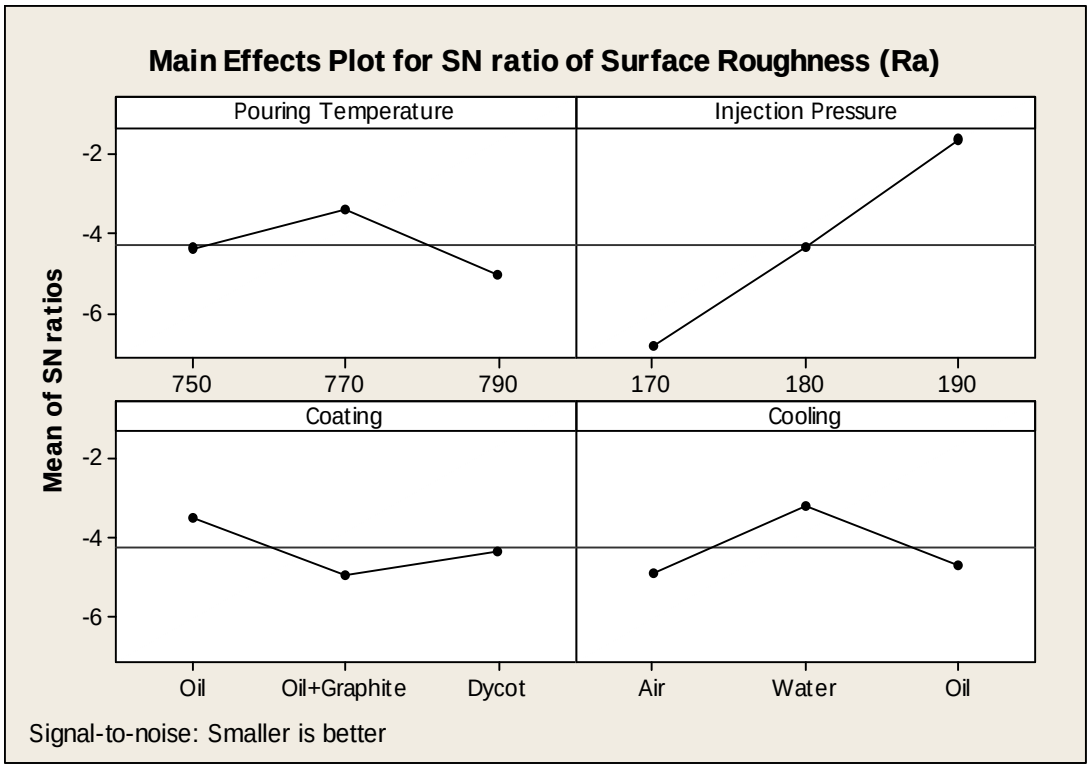


**Figure 4.2: Main effects Plot for S/N ratio of surface roughness**

## 4.5 OPTIMAL DESIGN FOR ROUGHNESS

The same level of all the significant factors provide a higher mean value and reduced variability so nothing has to be compromised. The level of factors which improves average and uniformity may conflict, so a compromise may have to be reached. Also a compromise

has to occur when multiple responses are considered and the same factor level may cause one response to improve and other to deteriorate [33].In this experimental analysis, the main effect plot in Figure 4.1 and estimate the mean surface roughness. From the, Table 4.6 it is concluded that lowest roughness was observed when injection pressure was kept at 190 kg/cm$^2$ .In S/N ratio lowest roughness was observed when injection pressure was kept at 190 kg/cm$^2$ ,pouring temperature at 770ºC and for cooling water was used during casting because these decrease variation.

Table 4.6 Significant Factors and Their Levels

| Factor | Affecting mean | | Affecting variation | |
|---|---|---|---|---|
| | Contribution | Best level | Contribution | Best level |
| Pouring Temperature, A | insignificant | - | significant | Level -2 ,(770ºC) |
| Injection Pressure, B | significant | Level-3, (190kg/cm$^2$) | significant | Level-3, (190kg/cm$^2$) |
| Coating, C | insignificant | - | insignificant | - |
| Cooling, D | insignificant | - | significant | Level-2 ,(Water) |

***Estimating the mean***

In experimental analysis, surface roughness is a lower average response is better (LB) characteristic. Depending on the characteristic, different treatment combinations has chosen to obtain satisfactory results. After conducting the experiments the optimum treatment condition within the experiments determined on the basis of prescribed combination of factor levels is determined to one of those in the experiment [36].

Mean value for Roughness

$$\mu_{A_2 B_3 D_2} = \overline{A_2} + \overline{B_3} + \overline{D_2} + - 2\overline{T}$$

$$= 1.585 + 1.242 + 1.538 - 2 \times 1.694 = 0.977\ micron$$

***Confidence Interval around the Estimated Mean***

The confidence interval is a maximum and minimum value between which the true average should fall at some stated percentage of confidence. The estimate of the mean μ is only a point estimate based on the averages of results obtained from the experiment. Statistically this provides a 50% chance of the true averages being greater than μ and a 50% chance of the true average being less than μ [36].

Confidence Interval around the estimated roughness mean

$$CI_1 = \sqrt{\frac{F_{\alpha,v_1,v_2} V_e}{n_{eff}}}$$

Where $F_{\alpha v_1 v_2} = F\ ratio$

$\alpha = risk$ (0.05) $\quad confidence = 1-\alpha$

$v_1 = dof\ for\ mean\ which\ is\ always = 1$

$v_2 = dof\ for\ error = v_e$

$n_{eff}$ = Number of tests under that condition using the participating factors

$$n_{eff} = \frac{N}{1 + dof_{A,B,D}} = \frac{9}{1+2+2+2} = 1.28$$

$$CI_1 = \sqrt{\frac{F_{\alpha,v_1,v_2} V_e}{n_{eff}}} = \sqrt{\frac{0.1 \times 0.0272}{1.28}} = 0.046$$

So, the confidence interval around the Surface Roughness is given by 0.977±0.046 micron.

## 4.6 RESULTS FOR DENSITY

The density of the cast material was obtained by using micrometer to conclude the volume and the weight was observed by using the electronic weighing scale available in metrology at Thapar University, Patiala. Density is denoted by $\rho = \frac{Weight}{volume}$ .The result for density for each of the 9 experiments is given in Table in 4.7.

**Table 4.7: Results for Density**

| Trial No. | Pouring temp. | Injection pressure | Coating type | Cooling type | Density(gms/mm$^3$) | | Mean density | S/N ratio |
|---|---|---|---|---|---|---|---|---|
| | | | | | I | II | | |
| 1 | $750^0$ | 170 | Oil Coating | Air Cooling | 2.300 | 2.300 | 2.3000 | 7.23456 |
| 2 | $750^0$ | 180 | Oil+ graphite | Water Coolig | 2.544 | 2.542 | 2.5430 | 8.10693 |
| 3 | $750^0$ | 190 | Dycot | Oil Cooling | 2.656 | 2.569 | 2.6125 | 8.33751 |
| 4 | $770^0$ | 170 | Oil+ graphite | Oil Cooling | 2.146 | 2.143 | 2.1445 | 6.62651 |
| 5 | $770^0$ | 180 | Dycot | Air Cooling | 2.307 | 2.307 | 2.3070 | 7.26095 |
| 6 | $770^0$ | 190 | Oil Coating | Water Coolig | 2.403 | 2.402 | 2.4025 | 7.61327 |
| 7 | $790^0$ | 170 | Dycot | Water Coolig | 2.222 | 2.224 | 2.2230 | 6.93879 |
| 8 | $790^0$ | 180 | Oil Coating | Oil Cooling | 2.586 | 2.590 | 2.5880 | 8.25928 |
| 9 | $790^0$ | 190 | Oil+ graphite | Air Cooling | 2.658 | 2.656 | 2.6570 | 8.48783 |

## 4.7 ANALYSIS OF VARIANCE- DENSITY

The results were analyzed using ANOVA for identifying the significant factor affecting the performance measures. ANOVA for the mean density at 95% confidence interval is given in Table 4.8. ANOVA table shows that injection pressure (F value (14.73) and pouring temperature (F value 6.57) are the factors that significantly affects the density. All other factors, namely, coating and cooling were found to be insignificant. Table 4.9 shows the rank of various factors in the term of their relative significance. Pressure has the highest rank, signifying highest contribution to density and the cooling has the lowest rank and was observed to be insignificant. Main effect plot for the mean density is shown in the Figure 4.3 which shows the density increase with the increase in injection pressure.

**Table 4.8: Analysis of Variance for Means density**

| Factors | SS | v | V | F | SS' | % Contribution |
|---|---|---|---|---|---|---|
| Pouring Temperature | 0.082106 | 2 | 0.041053 | 6.57 | 0.057114 | 20.48 |
| Injection Pressure | 0.184161 | 2 | 0.092080 | 14.73 | 0.159169 | 57.09 |
| Coating | 0.007292 | 2 | 0.003646 | | | |
| Cooling | 0.005204 | 2 | 0.002602 | | | |
| e-pooled | 0.012498 | 4 | 0.00646 | | | |
| Total | 0.278762 | 8 | | | | |

**Table 4.9: Response Table for Means for Density**

| Level | Temperature | Pressure | Coating | Cooling |
|---|---|---|---|---|
| 1 | 2.485 | 2.223 | 2.430 | 2.421 |
| 2 | 2.285 | 2.479 | 2.448 | 2.390 |
| 3 | 2.489 | 2.557 | 2.381 | 2.448 |
| Delta | 0.205 | 0.335 | 0.067 | 0.059 |
| Rank | 2 | 1 | 3 | 4 |

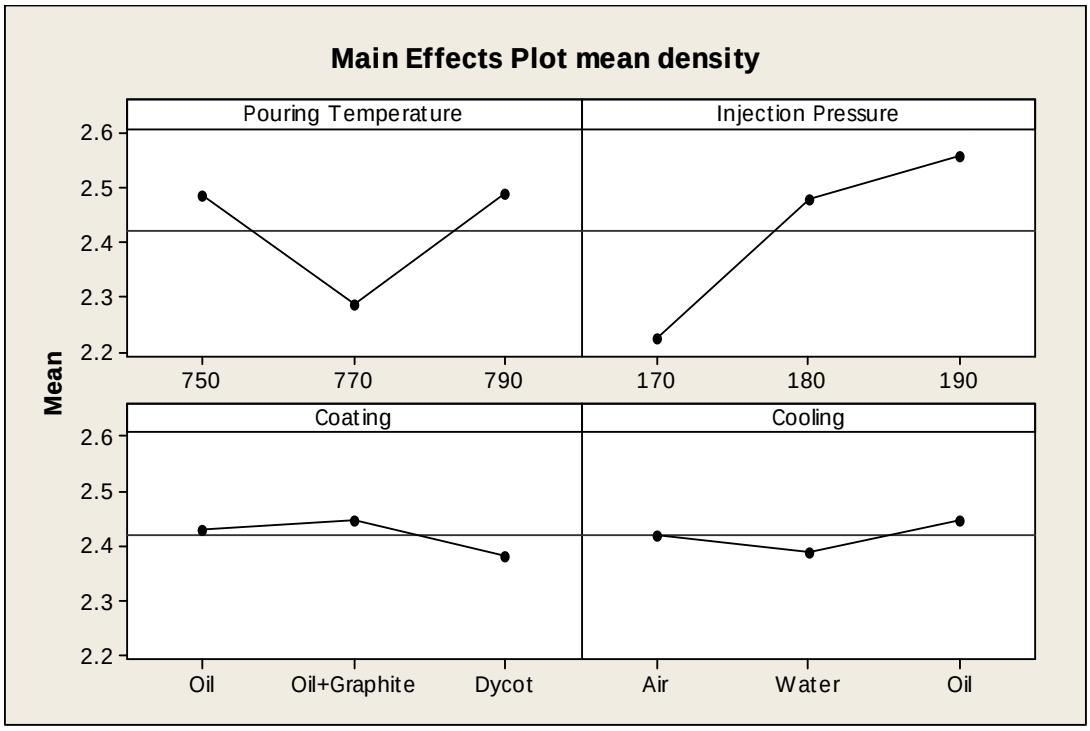


**Figure 4.3 Main effect plots for mean density**

## 4.8 RESULTS FOR S/N RATIO – DENSITY

The S/N ratios have been calculated to identify the major contributing factors and interactions that cause variation in density. Density a "Higher the better" type response is given by a logarithmic function based on the mean square deviation (MSD),

$(S/N)_{HB} = -10 \log (MSD_{HB})$

Where $MSD_{HB} = \frac{1}{r}\sum_{j=1}^{r}\left(\frac{1}{y_j^{\,2}}\right)$

$MSD_{HB}$ = Mean Square Deviation for higher-the-better response.

Table 4.10 shows the ANOVA results for S/N ratio of density at 95% confidence interval. Except coating and cooling factor, the other two factors pouring temperature and injection pressure were found to be significant. According to F-test injection pressure was observed to be the most significant factor affecting the density, followed by pouring temperature according to F-test. Main effect plot of S/N ratio for surface roughness are shown in the Figure 4.4.

**Table 4.10: Analysis of Variance for S/N ratio for Density**

| Factors | SS | V | V | F | SS' | % Contribution |
|---|---|---|---|---|---|---|
| Pouring Temperature | 1.05775 | 2 | 0.5288 | 7.396 | 0.77175 | 21.44 |
| Injection Pressure | 2.43251 | 2 | 1.21625 | 17.010 | 2.14651 | 59.07 |
| Coating | 0.08952 | 2 | 0.04476 | | | |
| Cooling | 0.05347 | 2 | 0.02674 | | | |
| e-pooled | 0.14299 | 4 | 0.0715 | | | |
| Total | 3.63325 | 8 | | | | |

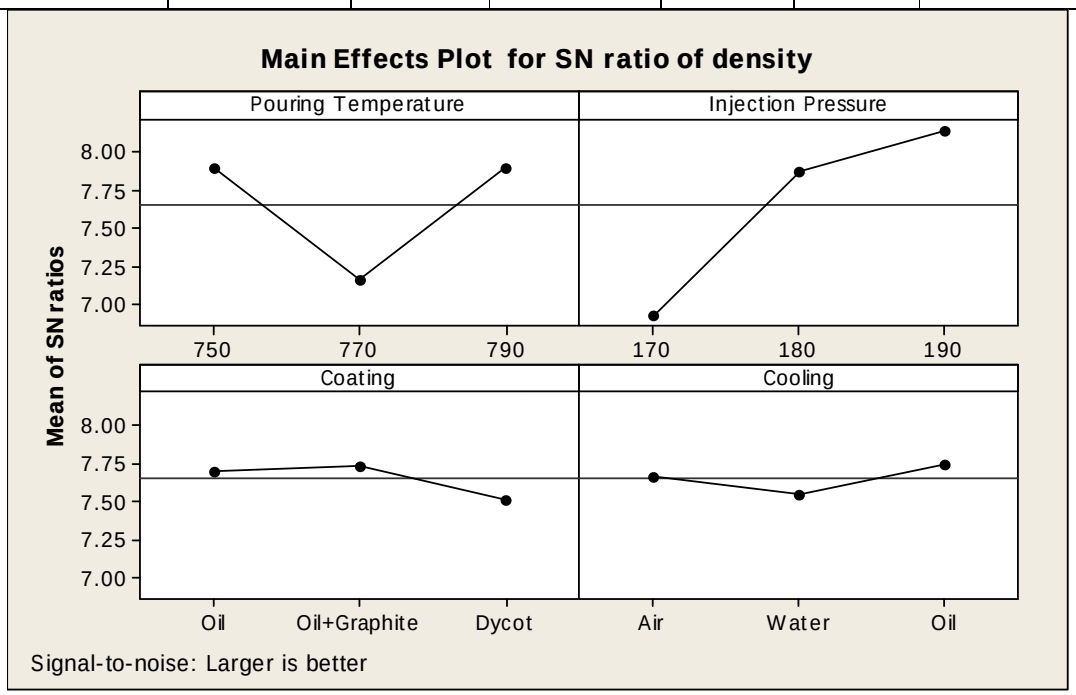


**Figure 4.4 Main effect plots for S/N Ratio of density**

## 4.9 OPTIMAL DESIGN FOR DENSITY

The same level of all the significant factors provide a higher mean value and reduced variability so nothing has to be compromised. In this experimental analysis, the main effect plot in Figure 4.3 and estimate the mean for density. From the, Table 4.11 it is concluded that highest density was observed when injection pressure was kept at 190 kg/cm$^2$ and pouring temperature at 790ºC .In S/N ratio plot 4.4 shows same result.

Table 4.11 Significant Factor and their Levels

| Factor | Affecting mean | | Affecting variation | |
|---|---|---|---|---|
| | Contribution | Best level | Contribution | Best level |
| Pouring Temperature, A | significant | Level -3 ,(790ºC) | significant | Level -3 ,(790ºC) |
| Injection Pressure, B | significant | Level-3, (190kg/cm$^2$) | significant | Level-3, (190kg/cm$^2$) |
| Coating, C | insignificant | - | insignificant | - |
| Cooling, D | insignificant | - | insignificant | - |

***Estimating the mean***

In experimental analysis, density is a higher average response is better (HB) characteristic. After conducting the experiments the optimum treatment condition within the experiments determined on the basis of prescribed combination of factor levels is determined to one of those in the experiment

Mean value for Density

$$\mu_{B_3A_3} = \overline{A_3} + \overline{B_3} + - \overline{T}$$

$$=2.489+2.557-2.419=2.627 \text{gms/mm}^3$$

***Confidence Interval around the Estimated Mean***

Confidence Interval around the estimated density mean

$$CI_1 = \sqrt{\frac{F_{\alpha,v_1,v_2} V_e}{n_{eff}}}$$

Where $F_{\alpha v_1 v_2} = F\ ratio$

$\alpha = risk\ (0.05)$ $\qquad confidence = 1-\alpha$

$v_1 = dof\ for\ mean\ which\ is\ always = 1$

$v_2 = dof\ for\ error = v_e$

$n_{eff}$ = Number of tests under that condition using the participating factors

$$n_{eff} = \frac{N}{1 + dof_{A,B}} = \frac{9}{1+2+2} = 1.8$$

$$CI_1 = \sqrt{\frac{F_{\alpha,v_1,v_2} V_e}{n_{eff}}} = \sqrt{\frac{0.2 \times 0.00646}{1.8}} = 0.026$$

So, the confidence interval around the Density is given by 2.627 ± 0.026gms/mm$^3$.

## 4.10 RESULTS OF HARDNESS

Hardness was measured on a Rockwell Hardness Tester, (model AVERY 6402) England, available at Mechanics of Solid lab, Thapar University, Patiala. The hardness measurement is dependent on the diameter of indentation on the samples. The indents formed in the pyramid shaped steel ball indenter were measured on B scale with a minor load of 10 kg for 20 Seconds. The result of hardness for each of the 9 experiments is given in Table in 4.12.

**Table 4.12: Results of Hardness**

| Trial No. | Pouring temp. | Injection pressure | Coating type | Cooling type | Hardness (HRN) | | Mean hardness | S/N ratio |
|---|---|---|---|---|---|---|---|---|
| | | | | | I | II | | |
| 1 | $750^0$ | 170 | Oil Coating | Air Cooling | 70.00 | 71.66 | 70.830 | -37.0049 |
| 2 | $750^0$ | 180 | Oil+ graphite | Water Coolig | 66.62 | 67.33 | 66.975 | -36.5184 |
| 3 | $750^0$ | 190 | Dycot | Oil Cooling | 67.33 | 68.66 | 67.995 | -36.6500 |
| 4 | $770^0$ | 170 | Oil+ graphite | Oil Cooling | 67.00 | 69.00 | 68.000 | -36.6511 |
| 5 | $770^0$ | 180 | Dycot | Air Cooling | 75.33 | 71.33 | 73.330 | -37.3089 |
| 6 | $770^0$ | 190 | Oil Coating | Water Coolig | 72.66 | 71.66 | 72.160 | -37.1661 |
| 7 | $790^0$ | 170 | Dycot | Water Coolig | 70.33 | 71.00 | 70.665 | -36.9842 |
| 8 | $790^0$ | 180 | Oil Coating | Oil Cooling | 69.33 | 71.00 | 70.165 | -36.9230 |
| 9 | $790^0$ | 190 | Oil+ graphite | Air Cooling | 70.66 | 71.66 | 71.160 | -37.0449 |

## 4.11 ANALYSIS OF VARIANCE- HARDNESS

The results were analyzed using ANOVA for identifying the significant factor affecting the performance measures. The analysis of variance (ANOVA) for the mean hardness at 95% confidence interval is given in Table 4.13. ANOVA table shows that cooling (F value 28.58) pouring temperature (F value 20.03), and coating (F value 17.06) are the factor that significantly affects the hardness, whereas injection pressure was found to be insignificant. Table 4.14 shows the rank of various factors in the term of their relative significance. Cooling has the highest rank; signifying highest contribution to hardness and the pressure has the lowest rank and was observed to be insignificant in affecting hardness. Main effect plot for the mean hardness is shown in the Figure 4.5 which shows hardness increase with the increase in injection pressure.

**Table 4.13: Analysis of Variance for Mean Hardness**

| Factors | SS | v | V | F | SS' | % contribution |
|---|---|---|---|---|---|---|
| Pouring Temperature | 11.0780 | 2 | 5.53901 | 20.03 | 10.525 | 29.86 |
| Injection Pressure | 0.5530 | 2 | 0.27650 | | | |
| Coating | 9.4354 | 2 | 4.71770 | 17.06 | 8.882 | 25.20 |
| Cooling | 14.1806 | 2 | 7.9031 | 28.58 | 13.62 | 38.66 |
| e-pooled | 0.5530 | 2 | 0.27650 | | | |
| Total | 35.2471 | 8 | | | | |

**Table 4.14: Response Table for Means for hardness**

| Level | Temperature | Pressure | Coating | Cooling |
|---|---|---|---|---|
| 1 | 68.60 | 69.83 | 71.05 | 71.77 |
| 2 | 71.16 | 70.16 | 68.71 | 69.93 |

| | | | | |
|---|---|---|---|---|
| 3 | 70.66 | 70.44 | 70.66 | 68.72 |
| Delta | 2.56 | 0.61 | 2.34 | 3.05 |
| Rank | 2 | 4 | 3 | 1 |

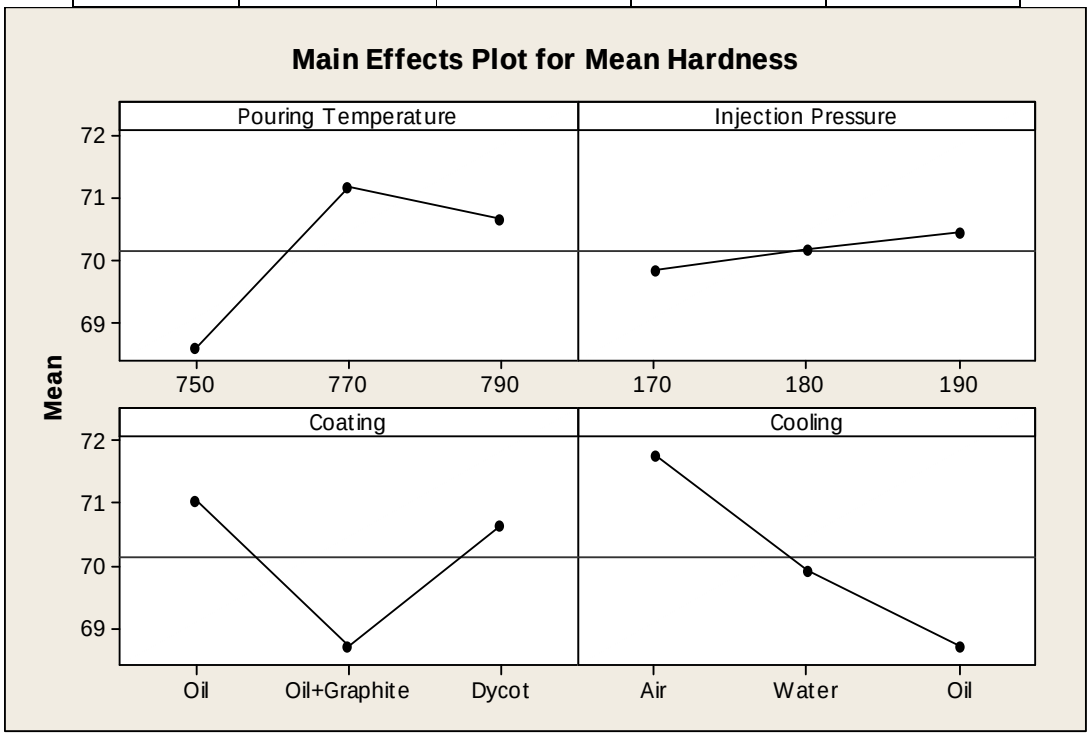


**Figure 4.5: Main effects plot for mean hardness**

## 4.13 RESULTS FOR S/N RATIO – HARDNESS

The S/N ratio consolidated several repetitions into one value and is an indication of the amount of variation present in the process. The S/N ratios have been calculated for hardness to identify the major contributing factors and interactions that cause variation in hardness. Hardness is a "lower the better" type response is given by a logarithmic function based on the mean square deviation (MSD),

$$S/N_{LB} = -10\log(MSD) = -10\log[(\frac{1}{r}\sum_{i=1}^{r} y^2{}_i)$$

Where $MSD_{LB} = \frac{1}{r}\sum_{j=1}^{r}\left(y_j{}^2\right)$

Table 4.15 shows the ANOVA results for S/N ratio of hardness at 95% confidence interval. Except injection pressure, all other factors are significant. According to F-test cooling was observed to be the most significant factor affecting the hardness, followed by pouring temperature and coating according to F-test. Table 4.15 shows the rank of various factors in the term of their relative significance. Cooling has the highest rank; signifying highest contribution to hardness and the pressure has the lowest rank and was observed to be insignificant in affecting hardness. Main effect plot of S/N ratio for hardness are shown in the Figure 4.6.

**Table 4.15: Analysis of Variance for S/N Ratio of Hardness**

| Factors | SS | V | V | F | SS' | % contribution |
|---|---|---|---|---|---|---|
| Pouring Temperature | 0.171647 | 2 | 0.085824 | 21.12 | 0.1635 | 29.99 |
| Injection Pressure | 0.008124 | 2 | 0.004062 | | | |
| Coating | 0.147499 | 2 | 0.073749 | 18.15 | 0.1393 | 25.56 |
| Cooling | 0.217914 | 2 | 0.108957 | 26.82 | 0.2097 | 38.48 |
| e-pooled | 0.008124 | 2 | 0.004062 | | | |
| Total | 0.545185 | 8 | | | | |

**Table 4.16: Response Table for S/N Ratio of Hardness**

| Level | Temperature | Pressure | Coating | Cooling |
|---|---|---|---|---|
| 1 | -36.72 | -36.88 | -37.03 | -37.12 |

| | | | | |
|---|---|---|---|---|
| 2 | -37.04 | -36.92 | -36.74 | -36.89 |
| 3 | -36.98 | -36.95 | -36.98 | -36.74 |
| Delta | 0.32 | 0.07 | 0.29 | 0.38 |
| Rank | 2 | 4 | 3 | 1 |

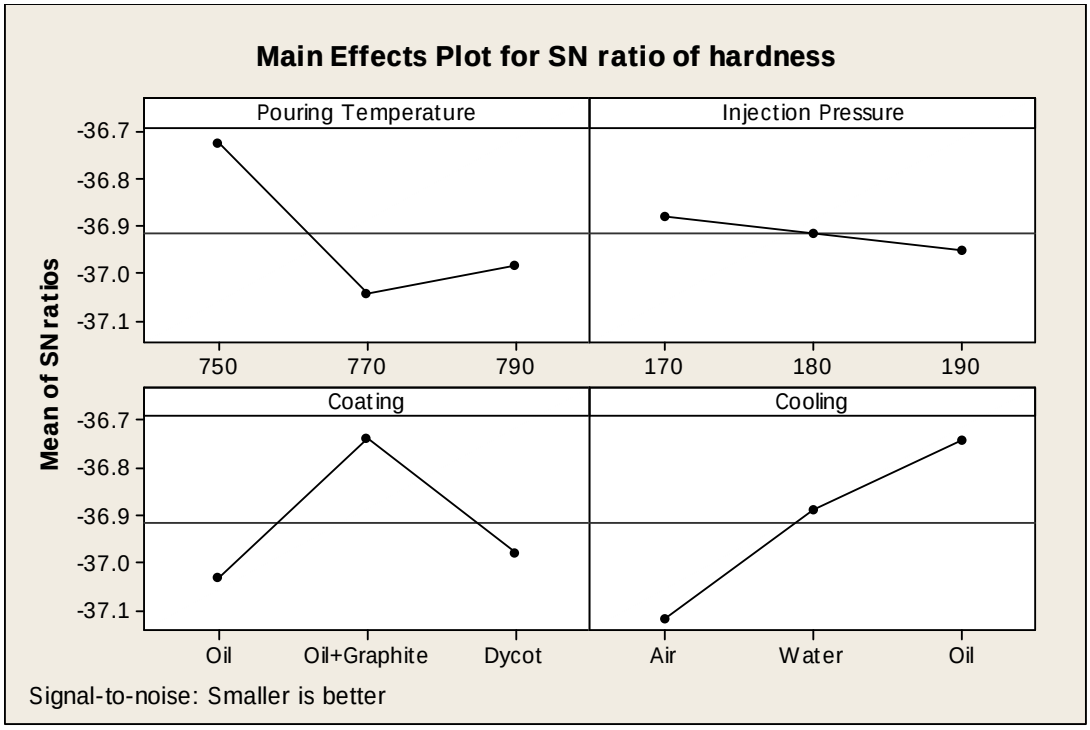


**Figure 4.6: Main Effect Plot for S/N Ratio of Hardness**

## 4.5 OPTIMAL DESIGN FOR HARDNESS

In this experimental analysis, the main effect plot in Figure 4.5 and estimate the mean surface roughness. From the, Table 4.17 it is concluded that lowest hardness was observed when roughness was observed when injection pressure was kept at pouring temperature at 750ºC and for cooling oil and oil–graphite coating was used during casting because these decrease variation. Same results were observed from main effect plot of S/N ratio for hardness Figure 4.6.

Table 4.17 Significant Factors and Their Levels

| Factor | Affecting mean | | Affecting variation | |
|---|---|---|---|---|
| | Contribution | Best level | Contribution | Best level |
| Pouring Temperature, A | significant | Level -1 , (750ºC) | significant | Level -1 , (750ºC) |
| Injection Pressure, B | insignificant | - | insignificant | - |
| Coating, C | significant | Level-2, (Oil+ Graphite) | significant | Level-2, (Oil+ Graphite) |
| Cooling, D | significant | Level-3 ,(Oil) | significant | Level-3 ,(Oil) |

***Estimating the mean***

Mean value for Hardness

$$\mu_{A_1C_2D_3} = \overline{A_1} + \overline{C_2} + \overline{D_3} + -2\overline{T}$$

$$= 68.58 + 68.72 + 68.72 - 2*70.14 = 65.74 \text{HRN}$$

***Confidence Interval around the Estimated Mean***

Confidence Interval around the estimated hardness mean

$$CI_1 = \sqrt{\frac{F_{\alpha, v_1, v_2} V_e}{n_{eff}}}$$

Where $F_{\alpha v_1 v_2} = F\ ratio$

$\alpha = risk$ (0.05) $\quad confidence = 1 - \alpha$

$v_1 = dof\ for\ mean\ which\ is\ always = 1$

$v_2 = dof\ for\ error = v_e$

$n_{eff}$ = Number of tests under that condition using the participating factors

$$n_{eff} = \frac{N}{1 + dof_{A,B,D}} = \frac{9}{1 + 2 + 2 + 2} = 1.28$$

$$CI_1 = \sqrt{\frac{F_{\alpha, v_1, v_2} V_e}{n_{eff}}} = \sqrt{\frac{0.1 \times 0.2750}{1.28}} = 0.1236$$

So, the confidence interval around the hardness is given by 65.74±0.12 HRN.

# CHAPTER 5

# EMPIRICAL MODELING

## 5.1 INTRODUCTION

Regression analysis is used to establish relationship between two variables. The response variable *y* is the independent variable or variable of interest, and the predictor variable *x* is the independent variable. An objective of regression analysis is to develop a regression model, relating *y* to *x* that can be used to predict values of the response variable. The regression was carried out using the MINITAB 15 software. An alpha level of 0.05 was used for all statistical tests

## 5.2 REGRESSION ANALYSIS FOR SURFACE ROUGHNESS

The regression analysis for surface roughness was done using MINITAB 15 software. The multifactor linear regression equation developed is shown in equation 5.1. In regression equation, T is representing temperature ($750^0$ C, $770^0$ C and $790^0$ C), P is representing pressure (170, 180 and190 kg/cm$^2$), Ct coating (i.e., 1 for oil, 2 for oil + graphite and 3 for dycote coating) and Cl cooling (1 for air cooling, 2 for water cooling and 3 for oil cooling). Where 8.52 is the constant term present in the equation. The predictor coefficient values and p values for all the predictors is shown in Table 5.1. The standard deviation of random error was found to be S = 0.227077 and R-Sq of the model was found to be R-Sq = 87.3%.

The regression equation is

Surface Roughness = 8.52 + 0.00233T - 0.0482 P + 0.0383 Ct - 0.0067 Cl

…… (equation 5.1)

**Table 5.1 Predictor Coefficient Table for Surface Roughness**

| Predictor | Coef | SE Coef | T | p |
|---|---|---|---|---|
| Constant | 8.516 | 3.949 | 2.16 | 0.097 |
| Temperature | 0.002333 | 0.004635 | 0.50 | 0.641 |
| Pressure | -0.048167 | 0.009270 | -5.20 | 0.007 |

| | | | | |
|---|---|---|---|---|
| Coating | 0.03833 | 0.09270 | 0.41 | 0.700 |
| Cooling | -0.00667 | 0.09270 | -0.07 | 0.946 |

## 5.3 REGRESSION ANALYSIS FOR DENSITY

The multifactor linear regression equation developed is shown in equation 5.2. In regression equation, T represents temperature ($750^0$ C, $770^0$ C and $790^0$ C), P represents pressure (170, 180 and190 kg/cm$^2$), Ct coating (i.e., 1 for oil, 2 for oil + graphite and 3 for dycote coating) and Cl cooling (1 for air cooling, 2 for water cooling and 3 for oil cooling). Where -0.56 is the constant term present in the equation. The predictor coefficient values and p values for all the predictors is shown in Table 5.2. The standard deviation of random error was found to be S = 0.161971 and R-Sq of the model was found to be R-Sq = 62.0% which suggest the good fit of the model. The temperature was omitted from the regression equation because of very high p value.

The regression equation is:

Density = - 0.56 + 0.0167P - 0.0250 Ct + 0.0133Cl

……. (equation 5.2)

**Table 5.2 Predictor Coefficient Table for Density**

| Predictor | Coef | SE Coef | T | p |
|---|---|---|---|---|
| Constant | -0.561 | 2.817 | -0.20 | 0.852 |
| Temperature | 0.00 | 0.003306 | 0.00 | 1.00 |
| Pressure | 0.016667 | 0.006612 | 2.52 | 0.065 |
| Coating | -0.02500 | 0.06612 | -0.38 | 0.725 |
| Cooling | 0.01333 | 0.06612 | 0.20 | 0.850 |

## 5.4 REGRESSION ANALYSIS FOR HARDNESS

The multifactor linear regression equation developed is shown in equation 5.3. In regression equation, T represents temperature ($750^0$ C, $770^0$ C and $790^0$ C), P represents pressure (170,

180 and190 kg/cm$^2$), Ct coating (i.e., 1 for oil, 2 for oil + graphite and 3 for dycote coating) and Cl cooling (1 for air cooling, 2 for water cooling and 3 for oil cooling). Where 28.4 is the constant term present in the equation. The predictor coefficient values and p values for all the predictors is shown in Table 5.3. The standard deviation of random error was found to be S = 1.87862 and R-Sq of the model was found to be R-Sq = 60.0%.

The regression equation is:

Hardness = 28.4 + 0.0517 T + 0.0302 P - 0.195 Ct - 1.53 Cl

…….. (equation 5.3)

**Table 5.3 Predictor Coefficient Table for Hardness**

| Predictor | Coef | SE Coef | T | p |
|---|---|---|---|---|
| Constant | 28.36 | 32.67 | 0.87 | 0.434 |
| Temperature | 0.05167 | 0.03835 | 1.35 | 0.249 |
| Pressure | 0.03025 | 0.07669 | 0.39 | 0.713 |
| Coating | -0.1950 | 0.7669 | -0.25 | 0.812 |
| Cooling | -1.5275 | 0.7669 | -1.99 | 0.117 |

# CHAPTER 6

# MULTI RESPONSE OPTIMISATION

## 6.1 INTRODUCTION

Chen has used Multi-Response Signal to Noise Ratio (MRSN) methodology to optimize various input parameters in a VLSI device. US Patent (Patent No.: US 6,546,522 B1, April 08, 2003) has been granted to this technique. This technique has been utilized for multi-response optimization.

Since there are two response parameters to be optimized, multiple S/N ratios are converted into a single value. In order to do this, it is important to normalize the S/N ratio of each response. Since S/N ratio is always targeted to be the highest for best performance, following equation is used to normalize the S/N ratio linearly:

$$\bar{s}_i = \frac{s_i - \min_i s_i}{\max_i s_i - \min_i s_i}$$

Where $s_i$ is the S/N ratio for $i^{th}$ trial for a particular response. In Table 2 S/N values for all the responses are given. Table 3 shows the normalized S/N ratios for Hardness, Density and Surface Roughness (Ra). The purpose of normalization is to convert the S/N ratio for the two responses into an equivalent responses scale where $\bar{s}_i$ will be unity for the best performance and zero for the worst for both type of response characteristic. For converting these multiple S/N responses into a single response which could be optimized, a multi-response S/N ratio (MRSN) was calculated of each trial condition. For achieving this, weight for each of the three responses was calculated. Procedure of assigning weight to the individual responses as under:

An appropriate Taguchi is used as a weight matrix for the experiment. This array is $L_9$, since in this situation there are only three responses to be optimised, a $L_9$ OA was an appropriate selection with four columns and nine rows representing nine trial conditions. All the three responses were treated as a control factor and were assigned to column 1, 2 and 3 of the $L_9$ matrix. The remaining column was left unassigned (denoted by 'e' as shown in Table 1).

The levels 1, 2 or 3 on the weight matrix representing the low, medium and high level of column were used to define the weight of the responses. The optimal weight-ratio of each experiment was obtained when MRSN is maximized by using Taguchi Method.

The MRSN was calculated by multiplying the individual normalized S/N ratio with the corresponding weight in the $L_9$ matrix used in this case and summing it for all the responses. The MRSN is thus given by:

$$\text{MRSN} = \sum_{i=1}^{4} w_i \bar{s}_i$$

Where MRSN is the multi-response S/N, $\bar{s}_i$ and $w_i$ are the individual normalized signal-to-noise ratio (S/N) and the respective assigned weight taken from the $L_9$ matrix.

**Table 6.1: L9 Orthogonal Array**

| Hardness | Density | Roughness | e |
|---|---|---|---|
| 1 | 1 | 1 | 1 |
| 1 | 2 | 2 | 2 |
| 1 | 3 | 3 | 3 |
| 2 | 1 | 2 | 3 |
| 2 | 2 | 3 | 1 |
| 2 | 3 | 1 | 2 |
| 3 | 1 | 3 | 2 |
| 3 | 2 | 1 | 3 |
| 3 | 3 | 2 | 1 |

**Table 6.2: S/N Ratio for all the Responses**

| Trial No. | Hardness | density | Roughness (Ra) |
|---|---|---|---|
| 1 | -37.00 | 7.23 | -6.81 |
| 2 | -36.26 | 8.11 | -4.05 |
| 3 | -36.65 | 8.34 | -2.31 |
| 4 | -36.65 | 6.63 | -7.04 |
| 5 | -37.31 | 7.26 | -4.19 |
| 6 | -37.17 | 7.61 | 1.06 |
| 7 | -36.98 | 6.94 | -6.59 |
| 8 | -36.92 | 8.26 | -4.79 |
| 9 | -37.04 | 8.49 | -3.72 |

**Table 6.3: Normalized Signal to Noise ratio for the responses** ('e' denotes the empty column).

| Normalized S/N of Hardness | Normalized S/N of Density | Normalized S/N of Surface Roughness (Ra) | E |
|---|---|---|---|
| 0.2907 | 0.3261 | 0.02889 | 0 |
| 1 | 0.7940 | 0.3688 | 0 |
| 0.6301 | 0.9177 | 0.5838 | 0 |
| 0.6290 | 0 | 0 | 0 |
| 0 | 0.3402 | 0.3531 | 0 |
| 0.1365 | 0.5292 | 1 | 0 |
| 0.3105 | 0.1675 | 0.0562 | 0 |
| 0.3690 | 0.8757 | 0.2786 | 0 |
| 0.2524 | 1 | 0.4099 | 0 |

## 6.2 MRSN SAMPLE CALCULATION FOR TRIAL 9

The $L_9$ weight matrix was assigned to trial 9 where the levels 1, 2 and 3 represent the respective weight for the column to which the three responses hardness, density and surface roughness (Ra) were assigned. The remaining column of the $L_9$ matrix was left unassigned and was denoted by e. The multiplication of individual S/N ratio to the levels representing weight resulted in a decision matrix as shown in Table 4. The MRSN was then obtained using the summation of outcome of the decision matrix and is shown in the last column of the decision matrix shown in the Table 4. The weight effect of responses at each level is then given in Table 5. The final maximum MRSN for trial 9 is then calculated using the additive model of Taguchi which in this trial is given by:

$$MRSN_{\text{trial 9}} = \overline{MRSN_{\text{hardness}}} + \overline{MRSN_{\text{density}}} + \overline{MRSN_{\text{roughness}}} - 2 \times T = 4.986808$$

Where $MRSN_{\text{hardness}}$, $MRSN_{\text{density}}$ and $MRSN_{\text{roughness}}$ represents the maximum mean multi-response S/N ratio for hardness, density and roughness, 3.577, 4.325 and 3.734 respectively.

## 6.3 MAXIMUM MRSN FOR ALL TRIALS

Using the above methodology, MRSN for each trial condition was calculated and is presented in Table 6. The mean values (at each level) for all the four factors for MRSN with their significance rank were shown in Table 7. Last row of these tables show the rank of each which implies the level of

significance of the factor on response. Rank 1 is the most significant factor and rank 4 is the least significant. The results were analyzed using Analysis of Variance (ANOVA) for identifying the significant affecting the MRSN and are presented in Table 8. The last column of ANOVA table show the F value for each factor. The principle of the F test is that the larger the F value for a particular parameter, the greater is its effect on response values.

**Table: 6.4 Normalized S/N ratio of responses converted to MRSN using $L_9$ OA as weight matrix** (sample calculations for 9th trial).

| Trial No. | Hardness | Density | Surface Roughness (Ra) | e |
|---|---|---|---|---|
| 1 | 0.2907 | 0.3261 | 0.0289 | 0 |
| 2 | 1 | 0.7940 | 0.3688 | 0 |
| 3 | 0.6301 | 0.9177 | 0.5838 | 0 |
| 4 | 0.6290 | 0 | 0 | 0 |
| 5 | 0 | 0.3402 | 0.3531 | 0 |
| 6 | 0.1365 | 0.5292 | 1 | 0 |
| 7 | 0.3105 | 0.1675 | 0.0562 | 0 |
| 8 | 0.3690 | 0.8757 | 0.2786 | 0 |
| 9 | 0.2525 | 1 | 0.4099 | 0 |

(Weight Matrix) W=

| Hardness | Density | Roughness | e |
|---|---|---|---|
| 1 | 1 | 1 | 1 |
| 1 | 2 | 2 | 2 |
| 1 | 3 | 3 | 3 |
| 2 | 1 | 2 | 3 |
| 2 | 2 | 3 | 1 |
| 2 | 3 | 1 | 2 |
| 3 | 1 | 3 | 2 |
| 3 | 2 | 1 | 3 |
| 3 | 3 | 2 | 1 |

Decision matrix

| Hardness | Density | Surface roughness | e | MRSN |
|---|---|---|---|---|
| 0.2525 | 1.0000 | 0.4098 | 0.0000 | 1.6623 |
| 0.2525 | 2.0000 | 0.8197 | 0.0000 | 3.0721 |
| 0.2525 | 3.0000 | 1.2295 | 0.0000 | 4.4820 |
| 0.5049 | 1.0000 | 0.8197 | 0.0000 | 2.3246 |
| 0.5049 | 2.0000 | 1.2295 | 0.0000 | 3.7344 |
| 0.5049 | 3.0000 | 0.4098 | 0.0000 | 3.9148 |
| 0.7574 | 1.0000 | 1.2295 | 0.0000 | 2.9869 |
| 0.7574 | 2.0000 | 0.4098 | 0.0000 | 3.1672 |
| 0.7574 | 3.0000 | 0.8197 | 0.0000 | 4.5771 |

**Table 6.5: Weight effect of each response at each level (sample representation for 9th trial)**

| Weight Level | Hardness | Density | Roughness |
|---|---|---|---|
| 1 | 3.072 | 2.325 | 2.915 |
| 2 | 3.325 | 3.325 | 3.325 |
| 3 | 3.577 | 4.325 | 3.734 |
| Max-Min | 0.505 | 2.000 | 0.820 |

**Table 6.6: Final MRSN corresponding to each trial**

| Trial | Normalized S/N of Hardness | Normalized S/N of Density | Normalized S/N of Roughness Ra | Final MRSN |
|---|---|---|---|---|
| 1 | 0.290714 | 0.326104 | 0.028881 | 1.9370 |
| 2 | 1 | 0.793965 | 0.368783 | 6.4870 |
| 3 | 0.630104 | 0.917628 | 0.583808 | 6.3948 |
| 4 | 0.629052 | 0 | 0 | 1.8872 |
| 5 | 0 | 0.340257 | 0.352098 | 2.0773 |
| 6 | 0.136559 | 0.52921 | 1 | 4.9979 |
| 7 | 0.31051 | 0.167479 | 0.056218 | 1.6026 |
| 8 | 0.369035 | 0.875672 | 0.27857 | 4.5699 |
| 9 | 0.252462 | 1 | 0.409836 | 4.9868 |

**Table 6.7: Response Table for MRSN (utilizing MRSN values from Table 6.6)**

| Level | Temp. | Pressure | Coating | Cooling |
|---|---|---|---|---|
| 1 | 4.940 | 1.809 | 3.358 | 3.000 |
| 2 | 2.987 | 4.378 | 4.454 | 4.284 |
| 3 | 3.720 | 5.460 | 3.835 | 4.363 |
| Delta | 1.952 | 3.651 | 1.095 | 1.362 |
| Rank | 2 | 1 | 4 | 3 |

**Table 6.8: Analysis of Variance for MRSN**

| Source | Degrees of freedom | Seq SS | Adj MS | F |
|---|---|---|---|---|
| Temperature | 2 | 5.8351 | 2.9176 | 3.2239 |
| Pressure kg/cm2 | 2 | 21.1001 | 10.5501 | 11.6576 |
| Coating | 2 | 1.8101 | 0.9050 | |
| Cooling | 2 | 3.5093 | 1.7546 | 1.9388 |
| Residual Error | 2 | 1.8101 | 0.9050 | |
| Total | 8 | 32.2546 | | |

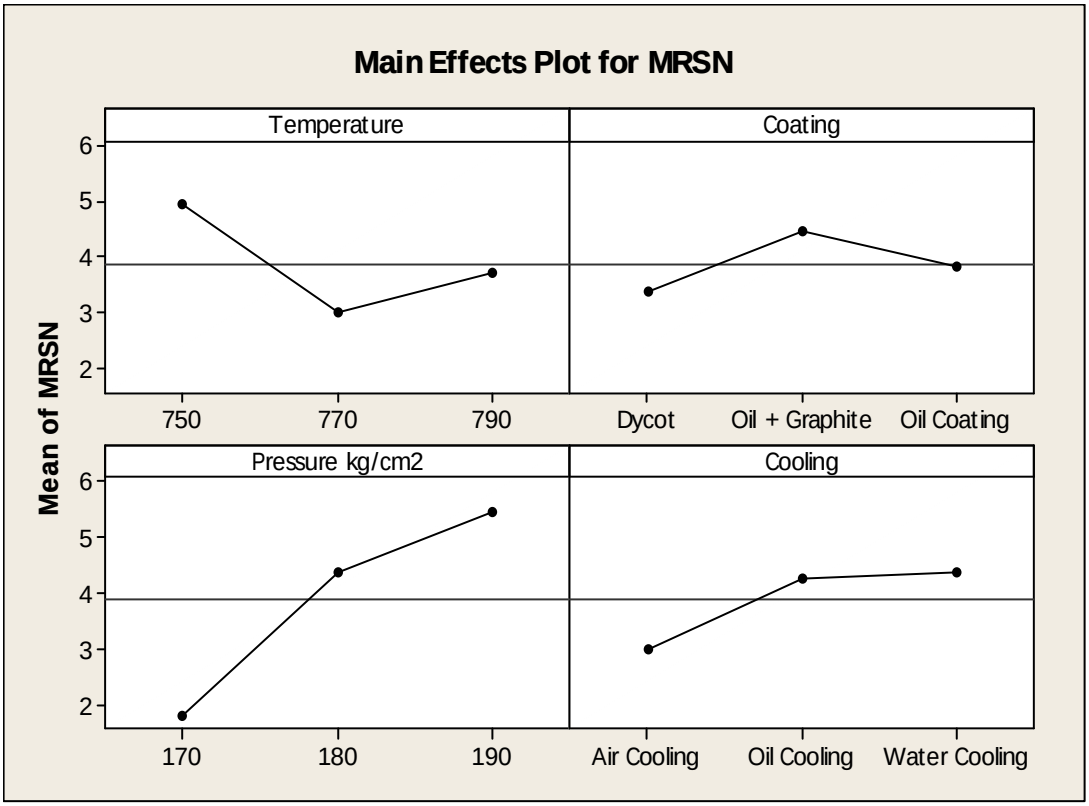


**Figure 6.1: Main Effect Plot For MRSN**

## 6.4 MAIN EFFECT PLOT

The main effect plots for MRSN ratio is shown in Figure 1. Main effect plots shows the variation of MRSN ratio for each factor i.e., temperature of the molten metal, injection pressure of the molten metal, type of coating and the type of cooling. The x- axis represents

the three levels at which each factor was varied and y axis shows the resultant change in MRSN ratio. The mean of response has been indicated by a horizontal line. One can observe from Figure 1, the MRSN ratio increases almost linearly with increase in injection pressure. The plots also indicated higher MRSN ratio with lower temperature i.e. at 750 degrees. Mean MRSN values at all the three levels are given in Table 7. The maximized MRSN ratio for all the trial conditions was then calculated using the Taguchi's additive model and is given by:

$$\text{MRSN} = \overline{MRSN}_{temperature_1} + \overline{MRSN}_{injectionpressure_3} + \overline{MRSN}_{coating_2} + \overline{MRSN}_{cooling_3} - 3 \times \overline{T} = 7.57$$

Where $\overline{MRSN}_{temperature_1}$ represents the maximum mean multi-response S/N ratio at level 1 for temperature = 4.940 (from Table 7) and so on. $\overline{T}$ is the mean of all MRSN = 3.88 as calculated from the last column of Table 7.

The maximized MRSN ratio obtained above represents the most optimal settings for the three contributing levels.

## 6.5 REGRESSION ANALYSIS FOR MRSN

The multiple factor regression analysis was done for MRSN. Predictor coefficient table along with p value is given in Table 9. Injection pressure was the only factor that comes out to be significant for MRSN. The regression equation was developed and is shown in equation 5.1. T represents temperature ($750^0$ C, $770^0$ C and $790^0$ C), P represents pressure (170, 180 and190 kg/cm$^2$), Ct coating (i.e., 1 for oil, 2 for oil + graphite and 3 for dycote coating) and Cl cooling (1 for air cooling, 2 for water cooling and 3 for oil cooing). Where 0.0305, 0.183 and 0.642 are the coefficients of temperature, injection pressure, coating and cooling respectively. Standard error was found to be 1.34314 and the R-Sq value was found to be 77.6%.

MRSN = - 6.3 - 0.0305 T + 0.183 P - 0.238 Ct + 0.642 Cl

……..…(equation 5.1)

**Table 6.9: Predictor Coefficient Table for MRSN**

| Predictor | Coef | SE Coef | T | p |
|---|---|---|---|---|

| | | | | |
|---|---|---|---|---|
| Constant | -6.30 | 23.36 | -0.27 | 0.801 |
| Temperature | -0.03050 | 0.02742 | -1.11 | 0.328 |
| Pressure | 0.18255 | 0.05483 | 3.33 | 0.029 |
| Coating | -0.2384 | 0.5483 | -0.43 | 0.686 |
| Cooling | 0.6418 | 0.5483 | 1.17 | 0.307 |

# CHAPTER 7

# MICROSTRUCTURE ANALYSIS

## 7.1 INTRODUCTION

LM6 exhibits excellent resistance to corrosion under both ordinary atmospheric and marine conditions. For the severest conditions this property can be enhanced by anodic treatment. The aluminium-silicon alloys possess exceptional casting characteristics, which enable them to be used to produce intricate castings of thick and thin sections. Fluidity and freedom from hot tearing increase with silicon content and are excellent throughout the range. The ductility of LM6 alloy enables castings to be easily rectified or modified in shape, e.g., simple components may be cast straight, and later bent to the required contour. LM6 is especially suited to castings that need to be welded although special care is needed when machining.

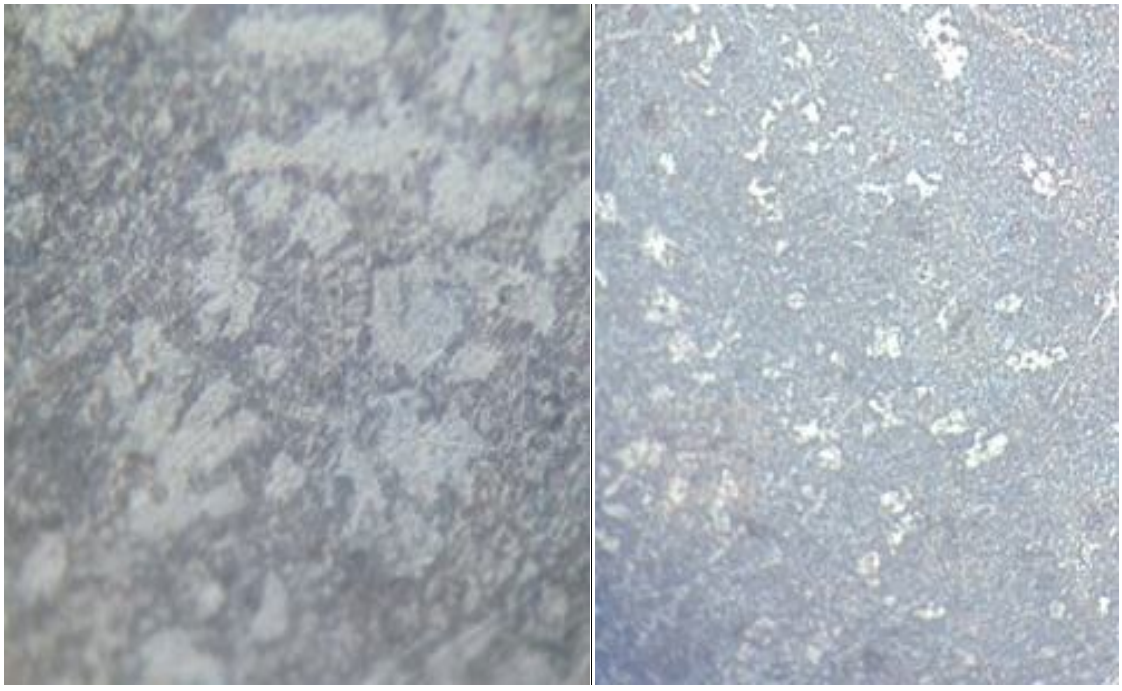

**Figure 7.1 Microstructure of LM6, Pouring Temperature $750^0$ , and Injection pressure 170 Kg/cm$^2$, Oil Coating, Air Cooling.**

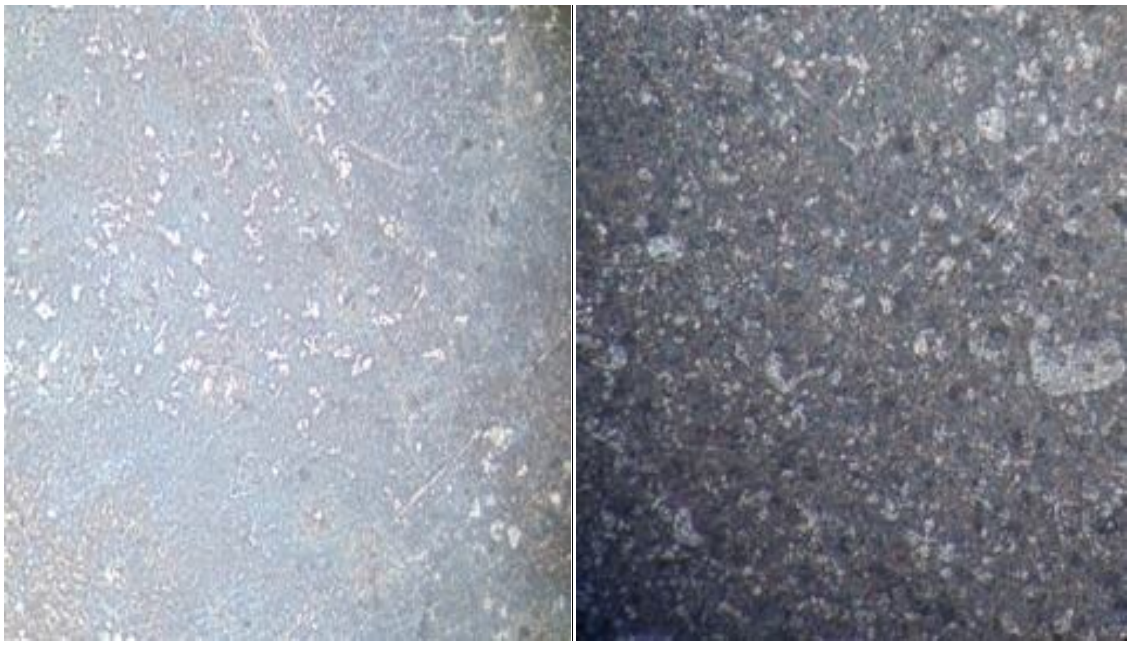

**Figure 7.2 Microstructure of LM6, Pouring Temperature $750^0$, and Injection pressure 180 $Kg/cm^2$, Oil Graphite Coating, Water Cooling.**

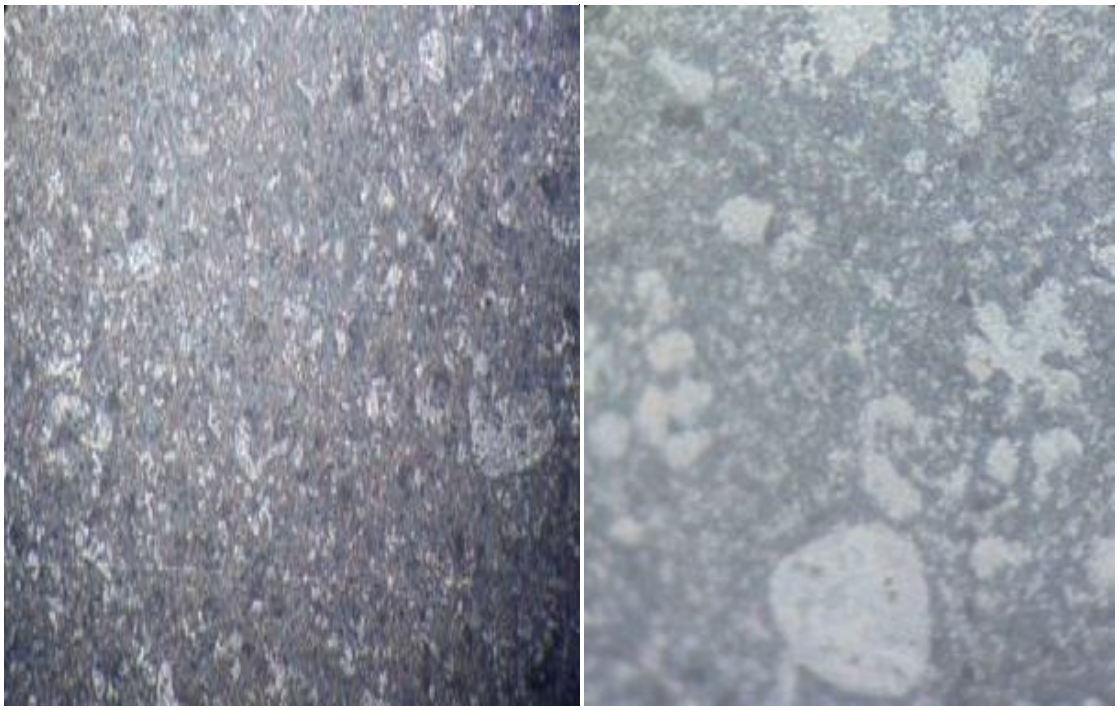

**Figure 7.3 Microstructure of LM6, Pouring Temperature $750^0$, and Injection pressure 190 $Kg/cm^2$, Dycot Coating, Oil Cooling.**

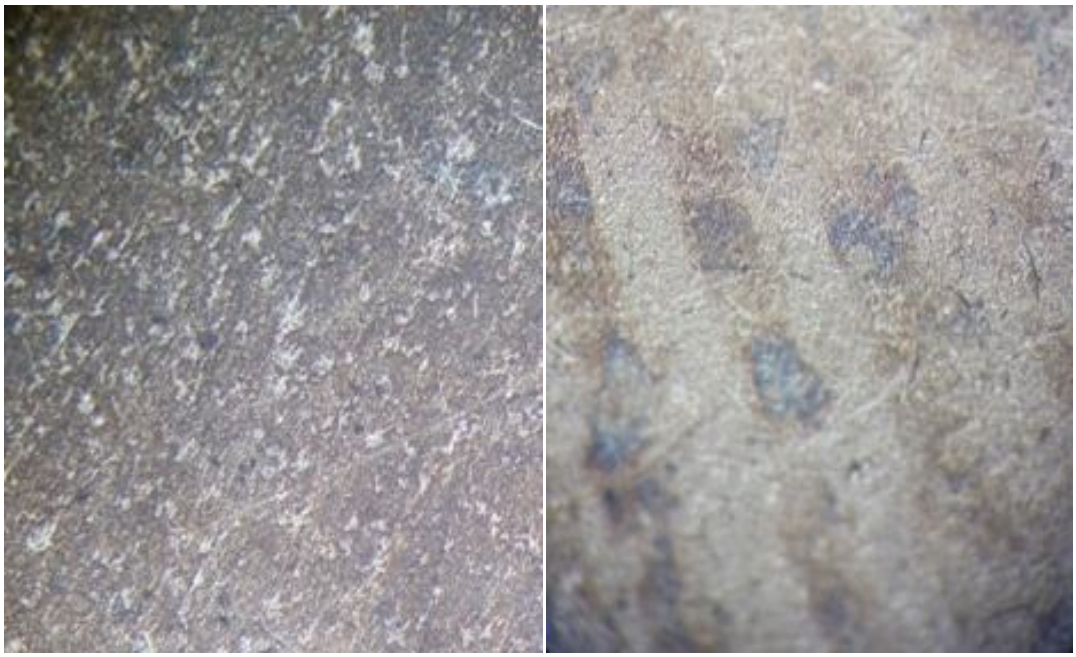

**Figure 7.4 Microstructure of LM6, Pouring Temperature $770^0$, and Injection pressure 170 Kg/cm$^2$, Oil Graphite Coating, Oil Cooling.**

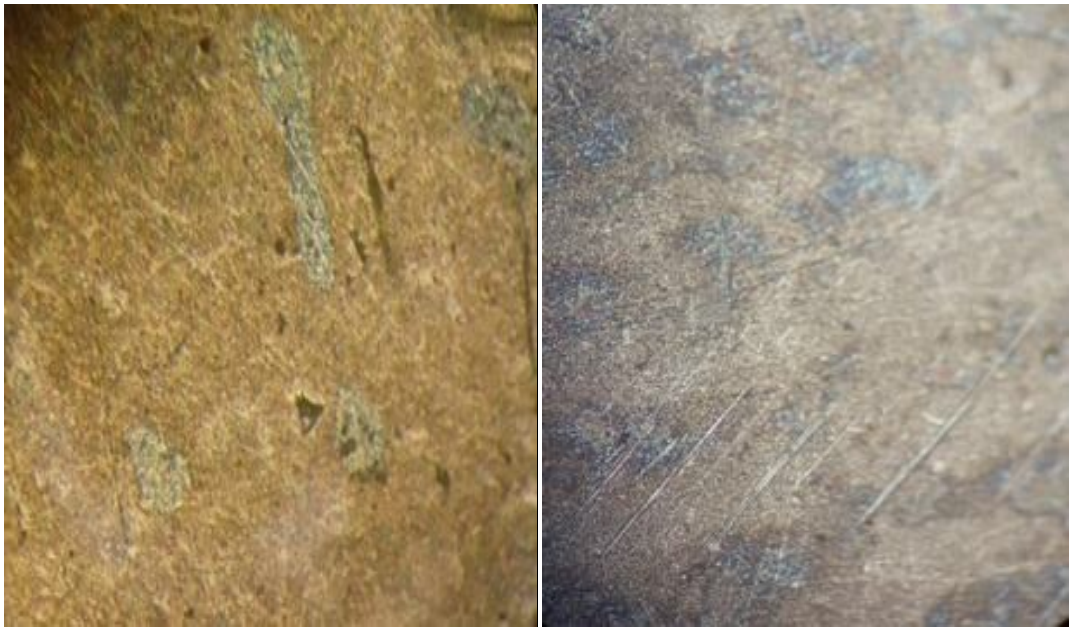

**Figure 7.5 Microstructure of LM6, Pouring Temperature $770^0$, and Injection pressure 180 Kg/cm$^2$, Dycot Coating, Air Cooling.**

**Figure 7.6 Microstructure of LM6, Pouring Temperature $770^0$, and Injection pressure 190 Kg/cm$^2$, Oil Coating, and Water Cooling.**

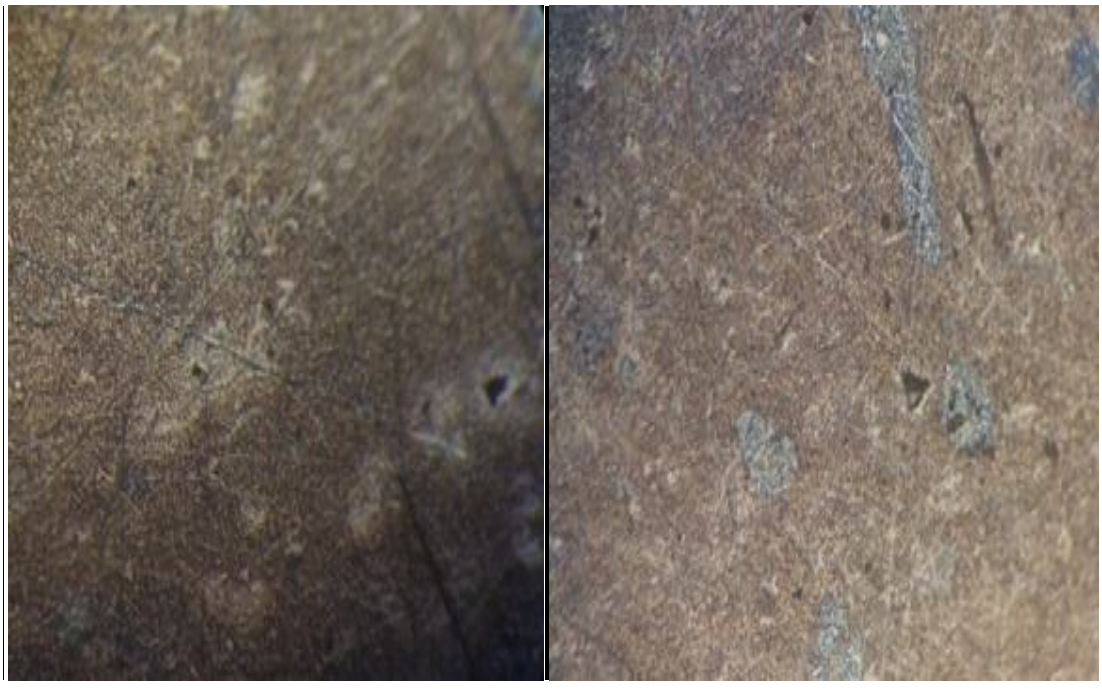

**Figure 7.7 Microstructure of LM6, Pouring Temperature $790^0$, and Injection pressure 170 Kg/cm$^2$, Dycot Coating, Water Cooling.**

**Figure 7.8 Microstructure of LM6, Pouring Temperature $790^0$, and Injection pressure 180 $Kg/cm^2$, Oil Coating, Oil Cooling.**

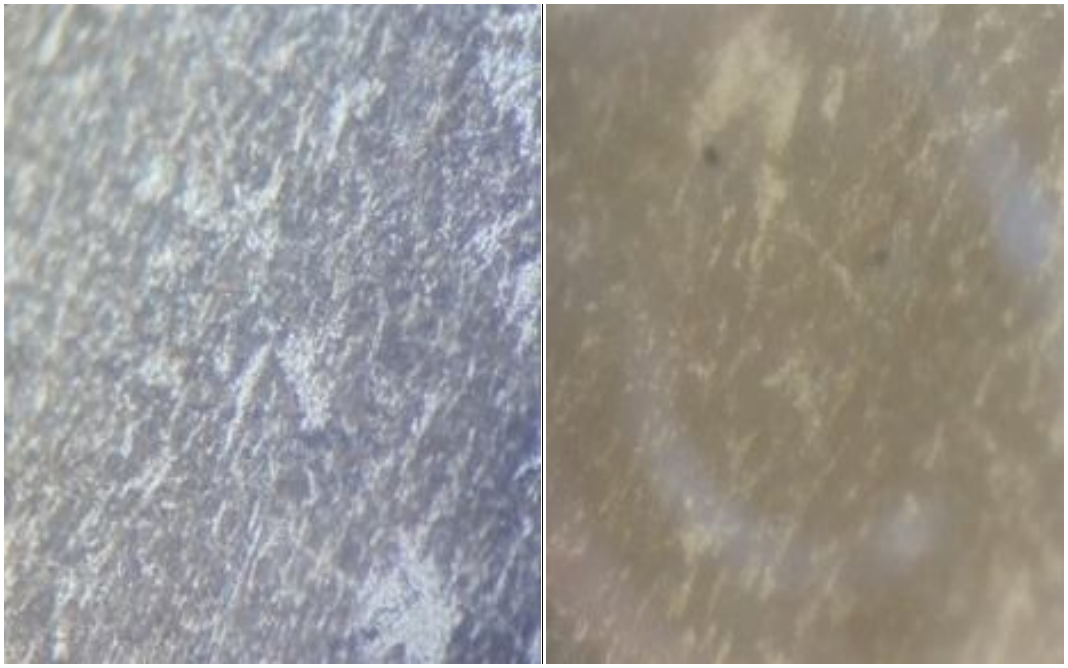

**Figure 7.9 Microstructure of LM6, Pouring Temperature $790^0$, Injection pressure 190 $Kg/cm^2$, Oil Graphite Coating, Air Cooling**

## 7.2 MICROSTRUCTURE ANALYSIS

Microstructure of die cast components made aluminium LM6 alloy have been investigated by means of Leica Metallurgical Microscope available at Thapar University, Patiala **.** The effects of parameters i.e. thermal characteristics (temperature of the molten metal), the injection pressure of the molten metal, type of coating (oil coating, oil + graphite coating, and dycot coating) on the microstructure of the cast product were observed on each of 9 experiments. The metallographic specimens were polished in usual manner with final polishing being carried out by hand, and they were etched in aqueous solution containing 2.5%$HNO_3$, 1.5 % HCL and 1% HF acid (etched with Keller's reagent) for about 20 seconds.

The phases present in die-cast alloy are aluminum in dendritic morphology, blocky and eutectic Silicon (sharp edges plate-shaped). The F block Si phase with generally circular shape is distributed in aluminum dendrites because of rapid solidification. The addition of $Al_2O_3$ particle to Al–Si alloy changed the size of aluminium dendrites and eutectic area morphology. The modification treatment causes the disappearance of primary silicon with the formation of solid solution dendrites (-Al) and fine globular eutectic silicon instead of needle like structures. It can be seen that due to modification in almost all the structures, the plate shaped primary silicon has disappeared from the structure and needle shaped eutectic silicon has become globular, while the iron rich Chinese script shaped-phase has transformed in to fine needle shaped –phase .

The LM6 alloy used for the experimental analysis was having 4% sodium. The structural modification of the alloy was done because of the presence of sodium. It has been observed from the previous studies that the addition of sodium or strontium to the melt results in modification due to change of eutectic silicon from plate-like to a branched fibrous form (ref). The morphology of the silicon has changed from a plate to a fibrous form as can be seen in the microstructure shown in Figure 7.1, Figure 7.3 and Figure 7.9 for the modified alloy. The primary silicon in the microstructure has completely disappeared due to suppression of the eutectic temperature, the eutectic point has been shifted to higher silicon content by the decrease of the eutectic temperature. Thus modification by metallic sodium has caused the alloy to become slightly hypoeutectic. The effect of modification due to sodium has slightly diminished due to oxidization because of open die casting process.

# CHAPTER 8

# RESULTS, CONCLUSIONS AND RECOMMENDATIONS

## 8.1 RESULTS

The effect of various input parameters i.e. thermal characteristics (temperature of the molten metal), injection pressure of the molten metal, type of coating (oil coating, oil+ graphite coating, dycot coating), and cooling medium (air cooling, water cooling and oil cooling) were evaluated using ANOVA and factorial design analysis. The purpose of the ANOVA was to identify the important parameters in prediction of surface roughness, density and hardness. The three responses were then converted to a single response using Multi-Response Signal to noise Ratio (MRSN) and were then evaluated using ANOVA to identify an optimal design for pressure Die Casting process. The results consolidated from ANOVA and plots are given below:

### 8.1.1 Surface Roughness

ANOVA analysis showed that injection pressure (F value 10.913) was the only factor that significantly affects the surface roughness. All other factors, namely, pouring temperature, coating and cooling were found to be insignificant. The injection pressure directly affects the quality of the surface produced and reduces porosity and other gas defects. It is concluded that lowest roughness was observed when injection pressure was kept at 190 kg/cm$^2$, pouring temperature at 770ºC and for cooling water was used during casting because these decreases variation. The estimated mean of surface roughness at the optimal level of all the factors at 95% confidence level was found to be 0.977 ± 0.046 micron.

For S/N ratio of surface roughness except coating, all other factors, namely, pressure temperature, injection pressure and cooling were found to be significant in affecting surface roughness ($R_a$).

### 8.1.2 Density

ANOVA table shows that injection pressure (F value (14.73) and pouring temperature (F value 6.57) are the factors that significantly affect density. The other two factors, namely, coating and cooling were found to be insignificant. It is concluded that highest density was observed when injection pressure was kept at 190 kg/cm$^2$ and pouring temperature at 790ºC.

For S/N ratio of density, except coating and cooling medium, the other two factors pouring temperature and injection pressure were found to be significant. The best value of density was observed with the 95% confidence level was 2.627 ± 0.026gms/$mm^3$.

### 8.1.3 Hardness

ANOVA table shows that cooling (F value 28.58) pouring temperature (F value 20.03), and coating (F value 17.06) are the factor that significantly affects the hardness, whereas injection pressure was found to be insignificant.

For S/N ratio of hardness, except injection pressure, all other factors are significant. According to F-test cooling was observed to be the most significant factor affecting the hardness, followed by pouring temperature and coating.

It is concluded that lowest hardness was observed when roughness was observed when injection pressure was kept at pouring temperature at 750ºC and for cooling oil and oil–graphite coating was used during casting because these decrease variation. The best value of hardness was observed with the 95% confidence level was 65.74 ± 0.12HRN.

## 8.2 MICROSTRUCTURE

1. Morphology of the silicon has changed from a plate to a fibrous form.
2. Structural change has been observed in almost all of microstructures. Structural modification of the alloy was done because of the presence of sodium
3. Addition of $Al_2O_3$ particle has changed the size of aluminium dendrites and eutectic area morphology.
4. Formation of solid solution dendrites (-Al) and fine globular eutectic silicon instead of needle like structures.
5. Primary silicon has disappeared from the structure and needle shaped eutectic silicon has become globular.
6. While the iron rich Chinese script shaped-phase has transformed in to fine needle shaped –phase.

## 8.3 MULTI-RESPONSE OPTIMIZATION

1. It was observed that MRSN ratio increases almost linearly with increase in injection pressure.
2. The plots also show that MRSN is maximized at low pouring temperature i.e. at 750 degrees.
3. Optimal results of MRSN were observed at $1^{st}$ level of temperature (750 degrees), third level of pressure (190 kg/$cm^2$, second level of coating (oil + graphite coating) and at third level of cooling medium (oil).

## 8.4 CONCLUSIONS

In the cold chamber high pressure die casting process aluminium alloy LM6, an experimental model for MRSN ratio encompassing three responses namely surface roughness, density and hardness has been employed to carry out the experimental study and subsequent analysis. The conclusions of the result are as follows.

- The result of ANOVA and the comparison of experimental data shows that the empirical model for MRSN are fairly well fitted with the experimental values with 95% confidence interval.
- The main significant factor in MRSN calculation is the injection pressure with F-value is equal to 11.56.
- The MRSN is maximized with increase in temperature and the cooling time. the MRSN is not affected by coating.
- The water cooling increased the hardness as compare to air and oil cooling.
- On increasing the pouring temperature of LM6 aluminium alloy a higher hardness was observed which could lead to some defects like cracking of the metal.
- It was concluded that in further studies the pouring temperature need not to be increased to higher temperatures. It was concluded from the study that higher injection pressures are more suitable in casting of aluminium alloys. Also, oil cooling is least preferred among the air and water cooling.
- From the analysis of microstructure of parts produced by cold chamber high pressure die casting process, structured changes have been observed in all samples because of presence of sodium. It is apparent that porosity present in a casting generally decreases as the pressure in the die casting increases. These trends confirm to the expected outcome.

## 8.5 RECOMMENDATIONS FOR FUTURE WORK

As the aluminum alloy has wide number of applications in automobile, aerospace, and many other manufacturing industries, but still not much work is available on its properties with different input process parameters. A rigorous study should be done to analyze the properties of aluminum alloys by varying process parameters and much work can be done in enhancing the properties of aluminium alloys.

## REFERENCES


1. North American Die Casting Association (2009), 241 Holbrook Drive, Wheeling, IL 60090
2. Copyright © 2009 eFunda, Inc.
3. ASM Handbook Volume 15, Casting (2008 Edition).
4. http://www.diecasting.org/faq/ downloaded on 15 March , 2010
5. DYCOT Manuals of Foseco GmbH, Germany.
6. http://www.kenwalt.com/DiecastingAlloys.pdf downloaded on 15 March, 2010.
7. http://www.custompartnet.com/wu/InjectionMolding downloaded on 15 March, 2010.
8. Hallam C.P. and Griffiths W.D., (2004), "A model of interfacial heat transfer coefficient for the aluminium die casting process", *Metallurgical and materials transactions B*, vol. 35B, pp. 723.
9. Zhi-Peng a Guo, Shou-Mei a Xiong, Bai-cheng a Liu, Bai-cheng a Liu, Li b Mei, Allison b Jhon.,(2008)"Determination of the heat transfer coefficient at metal-die interface of high pressure die casting process of AM50 alloy" *International journal of heat and mass transfer 51*, pp. 6032-6038.
10. Zhi-Peng a Guo, Shou-Mei a Xiong, Bai-cheng a Liu, Bai-cheng a Liu, Li b Mei, Allison b Jhon. (2008), "Effect of process parameter, casting thickness and alloys on the interfacial heat transfer coefficient in the high pressure die casting process" *Metallurgical and material transactions A, The minerals, metals and materials society and ASM international 2008. Vol.39A.pp. 2896*.
11. Zhi-peng GUO, Shoumei XIONG, SangHyun CHO and JeongKil CHOI.(2002), " Interfacial heat transfer coefficient between metal and die during high pressure die casting process of aluminium alloy" *Journal of materials processing technology. Pp.130-131, 299-303.*
12. Pearsson a Anders, Hogmark b Sture, Bergstrm a Jens.(2004), "Temperature profile and condition for thermal fatigue cracking in brass die casting dies" *Journal of materials processing technology 152.pp.228-236.*
13. Micowski J.R and Teufert C.E.,(), "The control of impact pressure in the pressure die casting process", *North America Die Casting Association.*

**14.** Matthew S, Dargusch a, Dourb G, Schauer c, Dinnis C.M. and Savaged G (2006), "The influence of pressure during solidification of high pressure die cast aluminium telecommunication components" *Journal of materials processing technology 180. Pp.37-43.*

***15.*** Chiang Ko-Ta, Liu Nun-Ming and Tsai Te-Chang. (2008) "Modelling and analysis of the effect of processing parameters on the performance characteristics in the high pressure die casting process of Al-Sl alloys". *Int J Adv Manuf Technol 41:1076-1084, Springer-Verlag London.*

**16.** "Final Report on Energy Consumption of Die Casting Operations", *US department of energy grant*/contract no. DE-FCo7-00ID13843.

**17.** Matthew Patrzalek, CRC CASTA/Prof. Ebrahim Shayan Dr. Dario Toncich Control of Cooling in Casting Dies, Based on Thermal Feedback

**18.** Yammagata H, Kasprzakb C., Aniolekb M, Kuritaa H and Sokolowskib J.H.(2008)"The effect of average cooling rates on the microstructure of Al-20% Si high pressure die casting alloy used for monolithic cylinder blocks " *Journal of materials processing technology 203.pp.333-341.*

**19.** Ahuett Horacio, Garza R, Miller Allen.,(2003), "The effect of heat released during fill on the deflection of die casting "*Journal of materials processing technology 142. Pp. 648-658.*

**20.** Han Q. And Vishvanathan S., (2003) ,"Analysis of the mechanism of die soldering in aluminium die casting", *Metallurgical and material transactions A,* vol. 34A, pp.139.

***21.*** Sumanth Shankar and Diran Apelian.,(2002)"Mechanism and preventive measures for die soldering during aluminium casting in a ferrous mould" JOM.

**22.** Hangi Yoshihiko and Utsunomiya Takao. (2009),"Fabrication of porous aluminium using gases intrinsically contained in aluminium alloy die casting" *The minerals, metals and materials society and ASM international 2009, 1284-vol.40A, Metallurgical and material transactions A.*

***23.*** Sabau A.S. and Vishvanathan S.,(2002)"Micro porosity prediction in aluminium alloy castings" *Metallurgical and materials transactions b Vol.33B.pp.243.*

**24.** Zhu J.D., Cockcroft S.L., and Maijer D.M.(2006)"Modelling of micro porosity formation in A 356 Aluminium Alloy Casting" *Metallurgical and materials transactions A. Vol. 37A.pp.1075.*

**25.** Zhua Hanliang, Guob Jingjie and Jiab Jun.,(2002), "Experimental study and theoretical analysis on die soldering in aluminium die casting" *Journal of materials processing technology 123. Pp.229-235.*

**26.** Hu Seyin Sevik, S. Can Kurnaz.(2006) , "Properties of alumina particulate reinforced aluminum alloy produced by pressure die casting, www.elsevier.com/locate/matdes, Materials and Design 27 (2006) 676–683

**27.** Kimuraa R, Yoshida M, Sasakia G, Panab J and Fucunagac H. (2002), "Influence of normal structure on the reliability of squeeze castings" *Journal of materials processing technology. Pp.130-131, 299-303.*

***28.*** Wei Ying-hui, Hou Li Feng, Yang Li-jing Xu Bing-she Kozuka Munehiro and Ichinose Hideki.(2009) "Microstructure and properties of die casting components with various thickness made of AZ91D alloy" *Journal of materials processing technology 209.pp.3278-3284.*

**29.** Yoshihiko Hangai a and Soichiro Kitahara b (2009), "Quantitative evaluation of porosity in aluminium alloy die castings by fractal analysis of spatial distribution of area" *Material and design 30.pp.1169-1173.*

***30.*** Kimuraa Ryosuke, Hatayamaa Haruaki, Shinozakia Kenji, Murashimab Izumi,Asadab Jo, Yoshidac Makoto., (2009), "Effect of grain refiner and grain size of susceptibility of Al-Mg die casting alloy to cracking during solidification", *Journal of materials processing technology 209.* pp.210-219.

**31.** Hong Soon-Jik and Suryanarayan C. (2005) "Mechanical properties and fracture behaviour of an ultrafine-grained Al-20 Wt Pct Si alloy" *Metallurgical and materials transactions A. Vol. 36A.pp.715.*

**32.** Blum W. Y.J.Li, Zeng X.H., Vongrobman B., and Haberling C.,(2005), "Creep deformation mechanism in High-pressure aluminium base alloys", *Metallurgical and material transactions A,* vol.36A,pp.1724.

**33.** http://www.kenwalt.com/DiecastingAlloys.pdf downloaded on 15 March, 2010.

**34.** The efficient application of die lubricant. *www.diecasting.org/dce*

**35.** Ross Phillip J., "Taguchi Techniques for Quality Engineering", McGraw-Hill, ISBN0-07-053866-2

**36.** K. Kocatepe and C. F. Burdett, (2000), "Effect of low frequency vibration on macro and microstructures of LM6 alloys," *Journal of Materials Science,*vol. 35, pp.3327 – 3335.